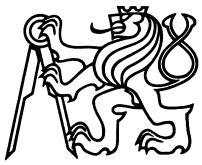

CZECH TECHNICAL UNIVERSITY IN PRAGUE
Faculty of Nuclear Sciences and Physical Engineering

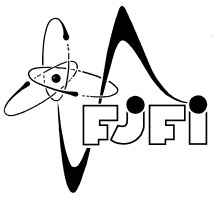

Dynamics of Two-dimensional Quantum Walks

Dynamika dvoudimenzionálních kvantových procházek

Research Project

Author: **Bc. Tereza Štefková**

Supervisor: **prof. Ing. Igor Jex, DrSc.**

Consultant: **Ing. Martin Štefaňák, Ph.D.**

Academic year: 2016/2017

Prohlášení

Prohlašuji, že jsem svůj výzkumný úkol vypracovala samostatně a použila jsem pouze podklady (literaturu, projekty, SW atd.) uvedené v přiloženém seznamu.

Nemám závažný důvod proti použití tohoto školního díla ve smyslu § 60 Zákona č. 121/2000 Sb., o právu autorském, o právech souvisejících s právem autorským a o změně některých zákonů (autorský zákon).

V Praze dne 30. 8. 2017 Tereza Štefková

Acknowledgment
I would like to express my honest gratitude to my supervisor prof. Igor Jex for suggesting this interesting topic and for his useful comments. I also thank my consultant Ing. Martin Štefaňák and Adrian Ortega for stimulating discussions.

Název práce:

Dynamika dvoudimenzionálních kvantových procházek

Autor: Bc. Tereza Štefková

Obor: Matematická fyzika

Druh práce: Research project

Vedoucí práce: prof. Ing. Igor Jex, DrSc., FJFI ČVUT

Konzultant: Ing. Martin Štefaňák, Ph.D., FJFI ČVUT

Abstrakt: Tato práce se zaměřuje převážně na speciální případ dvoudimenzionální kvantové procházky, totiž na dvoudimenzionální kvantovou procházku na takzvané Manhattanské mřížce.
Na úvod stručně shrneme problematiku dvoudimenzionálních kvantových procházek na kartézské mřížce s důrazem na efekt uvěznění. Poté zavedeme pojem klasické náhodné procházky na Manhattanské mřížce a její kvantové zobecnění. Nejdříve se budeme zabývat homogenní kvantovou procházkou na Manhattanské mřížce a odvodíme podmínky na mince, které vykazují efekt uvěznění.
Poslední kapitola je věnována studiu lokalizace v případě nehomogenních kvantových procházek na Manhattanské mřížce.

Klíčová slova: kvantová procházka, efekt uvěznění, Pólyovo číslo, Manhattanská mřížka

Title:

Dynamics of Two-dimensional Quantum Walks

Author: Bc. Tereza Štefková

Abstract : In this thesis we focus mainly on one special case of two-dimensional quantum walks, namely the two-dimensional quantum walks on the so-called Manhattan lattice.
We start with a brief summary of two-dimensional quantum walks on the Cartesian lattice with emphasis on the effect of trapping. Then we introduce the concept of a classical random walk on the Manhattan lattice and its quantum generalization. Firstly, we deal with the homogeneous quantum walks on the Manhattan lattice and derive the conditions on the trapping coins.
The last chapter is devoted to the study of the effect of localization in the case of the inhomogeneous quantum walks on the Manhattan lattice.

Key words: quantum walk, trapping effect, Pólya number, Manhattan lattice

Contents

Introduction **6**

1 Two-dimensional quantum walk on a lattice **7**
1.1 Time evolution 8
1.2 Effect of localization in quantum walks 9
1.3 Pólya number 10

2 Classical random walk on the Manhattan lattice **11**

3 Homogeneous quantum walk on the Manhattan lattice **12**
3.1 Time evolution 15
3.2 Trapping effect in quantum walks on the Manhattan lattice 16
3.3 Quantum walk on the Manhattan lattice with the Hadamard coin 18
3.3.1 Pólya number 19
3.4 Quantum walk on the Manhattan lattice with the rotation coin 21
3.5 Quantum walks on the finite Manhattan lattice 22
3.5.1 Absorbing boundaries 22
3.5.2 Periodic boundaries 24

4 Inhomogeneous quantum walk on the Manhattan lattice **29**
4.1 Absorbing boundaries 29

Conclusion **33**

Introduction

The concept of quantum walks, which can be viewed as quantum mechanical analogues of classical random walks, were first introduced by Aharanov *et al* [1] in 1993 and also studied by Meyer [2] in the context of quantum cellular automata. Research in this field has been gaining popularity recently mainly due to the potential utilization of quantum walks in quantum information theory and quantum computation.
One of the most remarkable achievements that motivated the study of quantum walks was the development of quantum algorithms based on quantum walks that are considerably better than their classical counterparts in terms of computational complexity. Among them, the most famous is the Grover search algorithm [3] that exhibits quadratic speed-up in comparison with the classical algorithms.
There have also been various experimental proposals and physical implementations of both quantum walks on a line and on a two-dimensional lattice using cold atoms in lattices, ion traps or polarization and orbital angular momentum of a photon (for a comprehensive review we recommend [4]).

The aim of this thesis is to study properties of discrete-time quantum walks on the so-called Manhattan lattice. They have been developed as a quantum generalization of the classical random walks on the Manhattan lattice that have been studied extensively in [5].
The motivation behind the study of quantum walks on lattices is to model transport in physical systems. We focus mainly on the so-called effect of localization, where the ballistic propagation of the quantum particle is suppressed. This corresponds to the transition from the conducting state of the material to the insulating state.
The thesis is organized as follows: In chapter 1 we briefly introduce the concept of a two-dimensional quantum walk on a Cartesian lattice and discuss those of its properties that will be relevant to the analysis of the quantum walks on the Manhattan lattice. Namely, we derive the time evolution using the method of the Discrete-Time Fourier Transform and focus on the effect of localization.
Chapter 2 deals with the classical random walks on the Manhattan lattice. We introduce the model used in [5] and summarize some of the results obtained there.
Chapter 3 is dedicated to homogeneous quantum walks on the Manhattan lattice. We describe them as homogeneous 8-state quantum walks on a Cartesian lattice which enables us to take advantage of the Discreet-Time Fourier Transform. We focus mainly on the effect of trapping and derive conditions on the trapping coins. We also comment on the special cases of the homogeneous quantum walks on the Manhattan lattice driven by the Hadamard coin and the rotation matrix. Second part of the third chapter focuses on quantum walks on the finite Manhattan lattice where both absorbing and periodic boundary conditions are taken into consideration.
In Chapter 4 we consider inhomogeneous quantum walks on the Manhattan lattice. We restrict ourselves only to time-homogeneous quantum walks with spatial inhomogeneity. Using numerical simulation we try to unravel the relation between the localization in the classical and quantum case.

Chapter 1

Two-dimensional quantum walk on a lattice

Let us now introduce the concept of a two-dimensional quantum walk on a Cartesian lattice. The position of the particle on the lattice is given by a vector from a Hilbert space $\mathcal{H}_p = \text{span}\{\,|p\rangle = |n,m\rangle \mid n,m \in \mathbb{Z}\}$, where n, m represent the coordinates on the lattice. The particle is assigned a Hilbert space $\mathcal{H} = \mathcal{H}_c \otimes \mathcal{H}_p$, where the Hilbert space $\mathcal{H}_c$ is the so-called coin space spanned by vectors

$$\{\,|R\rangle, |U\rangle, |L\rangle, |D\rangle\} = \left\{\begin{pmatrix}1\\0\\0\\0\end{pmatrix}, \begin{pmatrix}0\\1\\0\\0\end{pmatrix}, \begin{pmatrix}0\\0\\1\\0\end{pmatrix}, \begin{pmatrix}0\\0\\0\\1\end{pmatrix}\right\} \tag{1.1}$$

corresponding to all four possible directions of movement: to the right, up, to the left and down.
The time evolution of a quantum walk is realized by successive application of the evolution operator

$$U = S\,(C \otimes \mathbb{I}) \tag{1.2}$$

which comprises of two subsequent transformations of the state vector: the coin operator C acts solely on the coin state and S represents the conditional shift operator which takes the form of

$$\begin{aligned} S = \sum_{n,m\,\in\,\mathbb{Z}} \Big(&|R\rangle\langle R| \otimes |n+1,m\rangle\langle n,m| + |U\rangle\langle U| \otimes |n,m+1\rangle\langle n,m| \\ &+ |L\rangle\langle L| \otimes |n-1,m\rangle\langle n,m| + |D\rangle\langle D| \otimes |n,m-1\rangle\langle n,m| \Big). \end{aligned} \tag{1.3}$$

The state of the quantum walk after t steps with the normalized initial state localized at the origin

$$|\psi(0)\rangle = (\alpha\,|R\rangle + \beta\,|U\rangle + \gamma\,|L\rangle + \delta\,|D\rangle) \otimes |0,0\rangle\,, \qquad |\alpha|^2 + |\beta|^2 + |\gamma|^2 + |\delta|^2 = 1 \tag{1.4}$$

corresponds to

$$|\psi(t)\rangle = U^t\,|\psi(0)\rangle \tag{1.5}$$

$$= \sum_{n,m\,\in\,\mathbb{Z}} \Big(\psi_R(n,m,t)\,|R\rangle + \psi_U(n,m,t)\,|U\rangle + \psi_L(n,m,t)\,|L\rangle + \psi_D(n,m,t)\,|D\rangle\Big) \otimes |n,m\rangle\,, \tag{1.6}$$

where $\psi_j(n,m,t),\ j = R,U,L,D$ are components of the vector of the probability amplitudes $\psi(n,m,t)$ given as

$$\psi(n,m,t) = \begin{pmatrix}\psi_R(n,m,t)\\ \psi_U(n,m,t)\\ \psi_L(n,m,t)\\ \psi_D(n,m,t)\end{pmatrix} = \psi_R(n,m,t)\,|R\rangle + \psi_U(n,m,t)\,|U\rangle + \psi_L(n,m,t)\,|L\rangle + \psi_D(n,m,t)\,|D\rangle\,. \tag{1.7}$$

1.1 Time evolution

In the following we focus on the analysis of the time evolution of the quantum walks described above, i.e. we obtain general expressions for the probability amplitudes of the particle being at position $n,\ m$ at time t. We only consider homogeneous and time independent quantum walks (the coin operator C does not depend on $n,\ m,\ t$) since such types of walk are the most frequented ones and can be easily solved in the Fourier domain.

The desired time evolution can be written in the form of a recurrent relation

$$\psi(n,m,t) = C^1\psi(n-1,m,t-1) + C^2\psi(n,m-1,t-1) + C^3\psi(n+1,m,t-1) + C^4\psi(n,m+1,t-1) \quad (1.8)$$

with the initial condition

$$\psi(0,0,0) = (\alpha,\beta,\gamma,\delta)^T, \qquad |\alpha|^2 + |\beta|^2 + |\gamma|^2 + |\delta|^2 = 1 \quad (1.9)$$

where C^i corresponds to the coin operator C with zero elements except for the i-th row, i.e.

$$C^1 = \begin{pmatrix} c_{11} & c_{12} & c_{13} & c_{14} \\ 0 & 0 & 0 & 0 \\ 0 & 0 & 0 & 0 \\ 0 & 0 & 0 & 0 \end{pmatrix}, \quad C^2 = \begin{pmatrix} 0 & 0 & 0 & 0 \\ c_{21} & c_{22} & c_{23} & c_{24} \\ 0 & 0 & 0 & 0 \\ 0 & 0 & 0 & 0 \end{pmatrix} \quad (1.10)$$

$$C^3 = \begin{pmatrix} 0 & 0 & 0 & 0 \\ 0 & 0 & 0 & 0 \\ c_{31} & c_{32} & c_{33} & c_{34} \\ 0 & 0 & 0 & 0 \end{pmatrix}, \quad C^4 = \begin{pmatrix} 0 & 0 & 0 & 0 \\ 0 & 0 & 0 & 0 \\ 0 & 0 & 0 & 0 \\ c_{41} & c_{24} & c_{34} & c_{44} \end{pmatrix}. \quad (1.11)$$

Transforming the above recurrence using the Discrete-Time Fourier Transform

$$\tilde{f}(k,l) = \sum_{n,m\in\mathbb{Z}} f(n,m)\, e^{\mathrm{i}(k\,n+l\,m)}, \quad k,l \in [-\pi,\pi] \quad (1.12)$$

we obtain the time evolution in the Fourier domain in the following form (for detailed computation see[6])

$$\tilde{\psi}(k,l,t) = \tilde{U}(k,l)\,\tilde{\psi}(k,l,t-1) = \tilde{U}^t(k,l)\,\tilde{\psi}(k,l,0) \quad (1.13)$$

with the evolution operator in the Fourier domain given as

$$\tilde{U}(k,l) = \mathrm{diag}\left(\mathrm{e}^{\mathrm{i}k}, \mathrm{e}^{\mathrm{i}l}, \mathrm{e}^{-\mathrm{i}k}, \mathrm{e}^{-\mathrm{i}l}\right) C = \begin{pmatrix} e^{\mathrm{i}k} & 0 & 0 & 0 \\ 0 & e^{\mathrm{i}l} & 0 & 0 \\ 0 & 0 & e^{-\mathrm{i}k} & 0 \\ 0 & 0 & 0 & e^{-\mathrm{i}l} \end{pmatrix} \begin{pmatrix} c_{11} & c_{12} & c_{13} & c_{14} \\ c_{21} & c_{22} & c_{23} & c_{24} \\ c_{31} & c_{32} & c_{33} & c_{34} \\ c_{41} & c_{24} & c_{34} & c_{44} \end{pmatrix}. \quad (1.14)$$

As a result, the task of solving the recurrent relation (1.8) is reduced to that of finding the t-th power of $\tilde{U}(k,l)$ which is easily done when we diagonalize the evolution operator. The expression for the probability amplitudes in the Fourier domain then reads

$$\tilde{\psi}(k,l) = \sum_{j=1}^{4} \lambda_j^t(k,l) \left\langle \tilde{\psi}(k,l,0) \middle| v_j(k,l) \right\rangle v_j(k,l) \quad (1.15)$$

where λ_j are the eigenvalues of $\tilde{U}(k,l)$ and v_j are the corresponding eigenvectors. The $\langle .|. \rangle$ denotes the scalar product.
At this point we can return to the spatial domain using the Inverse Fourier Transform

$$f(n,m) = \frac{1}{(2\pi)^2} \int_{-\pi}^{\pi}\int_{-\pi}^{\pi} \tilde{f}(k,l)\, \mathrm{e}^{-\mathrm{i}(k\,n+l\,m)}\, \mathrm{d}k\, \mathrm{d}l \tag{1.16}$$

and obtain thus the analytic solution of the time evolution in the Cartesian coordinates as

$$\psi(n,m) = \frac{1}{(2\pi)^2} \sum_{j=1}^{4} \left(\int_{-\pi}^{\pi}\int_{-\pi}^{\pi} \lambda_j^t(k,l) \left\langle \tilde{\psi}(k,l,0) \middle| v_j(k,l) \right\rangle v_j(k,l)\, \mathrm{e}^{-\mathrm{i}(k\,n+l\,m)}\, \mathrm{d}k\, \mathrm{d}l \right). \tag{1.17}$$

1.2 Effect of localization in quantum walks

One of the interesting features of quantum walks is the so-called effect of localization when the particle has a non-vanishing probability to stay at the vicinity of the origin. There exist two types of localization in quantum walks; namely the trapping effect in the case of homogeneous quantum walks that stems from spectral properties of the evolution operators for special choices of the coin operator and the Anderson localization. The latter was first studied by Anderson in [7] who argued that electrons in a crystal become trapped when we apply external random potential on its atoms. Similar behaviour was observed for example in quantum walks driven by random matrices [8] or in the case of one-dimensional quantum walk homogeneous except for in the origin [9]. Let us now expand on the trapping effect.
For the majority of homogeneous two-dimensional quantum walks the probability of finding the particle at the fixed position converges to zero as number of steps t tends to infinity. This follows from the analogy with wave theory that was established in [10]. The authors derived the maximum group velocity that determines the propagation of the peaks in the probability distribution. The propagation stems from the continuous spectrum of the evolution operator $\tilde{U}(k,l)$.
However, there also exists quantum walks for which the discussed probability does not vanish. This remarkable feature termed as the trapping effect is closely related with the point spectrum of the quantum walk and depends on the choice of the coin operator.
In general, the eigenvalues of the coin operator can be written as $\lambda_j(k,l) = \mathrm{e}^{\mathrm{i}\omega_j(k,l)}$. The expression for the probability of finding the particle after t steps at the origin

$$P(0,t) = \sum_{j=1}^{4} \left(|\psi_R^j(0,t)|^2 + |\psi_U^j(0,t)|^2 + |\psi_L^j(0,t)|^2 + |\psi_D^j(0,t)|^2 \right) \tag{1.18}$$

consists of integrals containing eigenvalues $\lambda_j(k,l)$. From Riemann-Lebesgue lemma follows that only the expressions with eigenvalues λ_j independent of $k,\ l$ contribute to the probability $P(0,t)$ [11]. Hence the existence of constant eigenvalues implies the presence of the trapping effect. It can be easily proven that the general four-dimensional coin possesses either empty point spectrum or two constant eigenvalues in the form of $\pm\lambda$ [12].
At this point we note that the trapping effect is purely a quantum phenomenon without a classical analogue since the classical random walks diffuses in case of non-zero probability of leaving the current position. There is a remarkable difference between the trapping in one-dimensional and two-dimensional quantum walks. The latter allows for the trapping effect even in the case of a leaving walk. The extent of trapping also depends on the choice of the initial state, namely on the overlap between the initial state

and the eigenvectors corresponding to the constant eigenvalues. Initial states with zero overlap, i.e. orthogonal to these eigenvectors, lead to propagating walks.
A typical example of a trapping four-state quantum walk on a two-dimensional lattice is that of the Grover walk represented by the four-dimensional Grover coin

$$G = \frac{1}{2}\begin{pmatrix} -1 & 1 & 1 & 1 \\ 1 & -1 & 1 & 1 \\ 1 & 1 & -1 & 1 \\ 1 & 1 & 1 & -1 \end{pmatrix} \tag{1.19}$$

with one pair of constant eigenvalues ± 1 and two corresponding stationary states (for details see [13]). In this case, there exists only one initial state that is orthogonal to both of the stationary states, namely the state $\psi_G = \frac{1}{2}(1, -1, -1, 1)^T$ which results in a propagating quantum walk.
Notice that in case of one-dimensional quantum walks the trapping can always be avoided by one special choice of the initial state. On the contrary, four-dimensional trapping coins can be further classified as weakly trapping if the trapping effect can be avoided for a special choice of the initial state, or strongly trapping otherwise [14].

1.3 Pólya number

One of the interesting characteristics of quantum walks that is closely related to trapping is the probability of the eventual return to the origin. This property was first studied by Pólya [15] in connection with classical random walks. He introduced the so-called Pólya number according to which the quantum walks are classified as recurrent, if the Pólya number equals 1, or transient otherwise.
The Pólya number can be expressed in terms of the probability $p_0(t)$ of being at the origin at time t as

$$P = 1 - \frac{1}{\sum_{t=0}^{\infty} p_0(t)} \tag{1.20}$$

which leas us to a simple criterion: the random walk is recurrent if and only if $\sum_{t=0}^{\infty} p_0(t) = +\infty$.
The concept of Pólya number has been extended to quantum walks in [16]. The definition depends on the specification of the measurement scheme due to the quantum-mechanical nature of the particle. In [16] they use identically prepared states which they let evolve for t steps in the t-th trial before performing the measurement. This yields the following formula for the Pólya number

$$P = 1 - \prod_{t=1}^{\infty}(1 - p_0(t)). \tag{1.21}$$

At this point we note that in the case the functions $\omega(k, l)$ are smooth the asymptotic behaviour of the probability $p_0(t)$ can be estimated employing the method of stationary phase [16]. Notice that all trapping quantum walks are recurrent for every initial state that leads to trapped walk. Moreover, in contrast to classical random walks, that are recurrent only in dimensions 1 and 2 and where the Pólya number depends solely on the dimension of the lattice, we are able to construct recurrent quantum walks in arbitrary dimensions using a special choice of the coin operator [16].

Chapter 2

Classical random walk on the Manhattan lattice

In this chapter we introduce the model of classical random walks on the Manhattan lattice that is described in detail in [5].
The Manhattan lattice (see Figure 2) can be viewed as a two-dimensional Cartesian lattice with directed edges. At each node there are two incoming and two outgoing lines and the direction alternates both vertically and horizontally.
In the case of a classical random walk on this lattice there are scatterers placed randomly at each node with probability p and we assume the probability to be the same for all of the nodes. The walker moves according to the direction of the edges unless it encounters a scatterer. At a node with a scatterer it turns 90 degrees according to the orientation of the outgoing edges.
The classical random walk on the Manhattan lattice can be easily analysed for two special cases when there is a full absence or presence of the scatterers; i.e. the probability p is set to 0 and 1, respectively. The resulting classical random walks correspond to a walk with the walker propagating with the maximum velocity (after t steps its distance from the starting point is t) or it is trapped in a loop of length four.
In the next chapter be return briefly to the classical random walks on the Manhattan lattice to obtain the spectrum of these walks in case of full presence/absence of the scatterers using the methods described in the following. At this point we note that under specific conditions the Manhattan lattice can be viewed as two crossed Galton boards. We will expand on this in chapter 3.

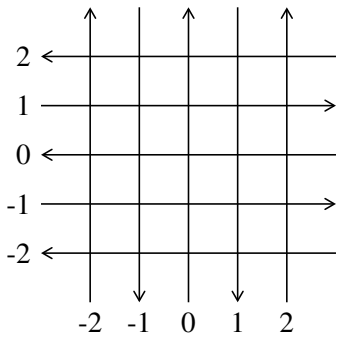

Figure 2.1: The Manhattan lattice.

Chapter 3

Homogeneous quantum walk on the Manhattan lattice

In the following we focus on quantum walks on the so-called Manhattan lattice as an extension of the classical model defined in the previous chapter.
Instead of scatterers we use two-dimensional coins at each node. The coin-state corresponds to the direction of motion, i.e. the orientation of the edges. The state of the whole system is described by a vector from Hilbert space $\mathcal{H} = \text{span}\{|R\rangle, |U\rangle, |L\rangle, |D\rangle\} \otimes \text{span}\{|x, y\rangle \, | x, y \in \mathbb{Z}\}$.
We use the following notation

$$\psi(x, y, t) = \begin{pmatrix} \psi_R(x, y, t) \\ \psi_U(x, y, t) \\ \psi_L(x, y, t) \\ \psi_D(x, y, t) \end{pmatrix} \tag{3.1}$$

for the probability amplitudes of being at node (x, y) at time t with the given state of the coin.

Our first aim is to construct a homogeneous quantum walk on the Manhattan lattice since it can be easily analysed with the help of the Fourier Transform.
However, in contrast to a quantum walk on a two-dimensional lattice described in the first chapter, a quantum walk on the Manhattan lattice cannot be homogeneous since the lattice itself is not. It can be readily seen that applying the same 4 dimensional unitary matrix C at each node yields in general superposition of all four basis states; however the conditional shift notices only two directions at each node. In other words, such a quantum walk would not be a unitary process.
However, it can be easily seen that the Manhattan lattice is homogeneous with respect to cells comprised of four nodes (Figure 3.1)). Let us now describe quantum walk on the Manhattan lattice with respect to these elementary Manhattan cells.
In the following we associate numbers 1, 2, 3 and 4 with nodes $|0, 0\rangle$, $|1, 0\rangle$, $|0, 1\rangle$ and $|1, 1\rangle$ (see Figure 3.1). Due to the direction of the edges we have to use four different coins at each node which can be expressed in the basis $\{|R\rangle, |U\rangle, |L\rangle, |D\rangle\}$ as

$$C_1 = \begin{pmatrix} 1 & 0 & 0 & 0 \\ 0 & a_1 & c_1 & 0 \\ 0 & b_1 & d_1 & 0 \\ 0 & 0 & 0 & 1 \end{pmatrix}, \quad C_2 = \begin{pmatrix} 1 & 0 & 0 & 0 \\ 0 & 1 & 0 & 0 \\ 0 & 0 & a_2 & c_2 \\ 0 & 0 & b_2 & d_2 \end{pmatrix}, \quad C_3 = \begin{pmatrix} a_3 & c_3 & 0 & 0 \\ b_3 & d_3 & 0 & 0 \\ 0 & 0 & 1 & 0 \\ 0 & 0 & 0 & 1 \end{pmatrix}, \quad C_4 = \begin{pmatrix} d_4 & 0 & 0 & b_4 \\ 0 & 1 & 0 & 0 \\ 0 & 0 & 1 & 0 \\ c_4 & 0 & 0 & a_4 \end{pmatrix}, \tag{3.2}$$

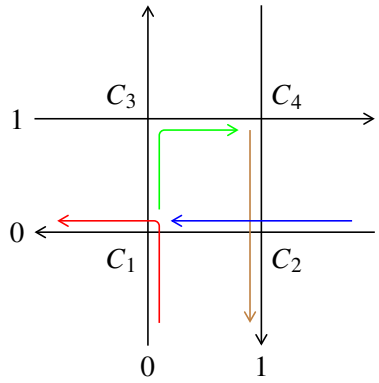

Figure 3.1: The elementary Manhattan cell.

where

$$\begin{pmatrix} a_j & c_j \\ b_j & d_j \end{pmatrix}, \quad j \in 1,2,3,4 \tag{3.3}$$

are arbitrary two-dimensional coins.
The position of the particle on the Manhattan lattice can be described by the position of the corresponding cell on the lattice (for this we use letters n, m), position of the node inside the cell (labelled by 1,2,3 or 4) and the coin state. In terms of (3.1) it means,

$$\psi(n,m,t) = \begin{pmatrix} \psi_1(n,m,t) \\ \psi_2(n,m,t) \\ \psi_3(n,m,t) \\ \psi_4(n,m,t) \end{pmatrix}, \text{ where } \quad \psi_i(n,m,t) = \begin{pmatrix} \psi_R(x,y,t) \\ \psi_U(x,y,t) \\ \psi_L(x,y,t) \\ \psi_D(x,y,t) \end{pmatrix}. \tag{3.4}$$

The state of the quantum walk is then described by a 16-component vectors $\psi(n,m,t)$. However, we will see that the number of components can be reduced to 8.
When describing one step of the quantum walk in a cell, we consider four possibilities (see Figure 3.1): the particle comes from outside of the cell and continues to another cell (red arrow), the particle comes from inside of the given cell and moves to another cell (brown arrow), the particle moves inside of the given cell (green arrow) and the particle comes from the outside and continues inside of the cell (blue). To describe this more effectively, we label the state by o and i which means that the particle comes from outside and inside of the cell, respectively.
The most general state of the quantum walk in the cell is then given by following linear combinations of coin states

$$\begin{aligned} &(0,0) : \alpha_1 |U\rangle_o + \alpha_2 |L\rangle_i \\ &(0,1) : \beta_1 |L\rangle_o + \beta_2 |D\rangle_i \\ &(1,0) : \gamma_1 |R\rangle_o + \gamma_2 |U\rangle_i \\ &(1,1) : \delta_1 |D\rangle_o + \delta_2 |R\rangle_i . \end{aligned} \tag{3.5}$$

It is easily seen that we do not have to specify the position of the node inside the cell since every combination of the coin state and state o or i is unique. In other words, there exists a bijection between relation (3.5) and eight-component vector

$$\psi(n,m,t) = \begin{pmatrix} \psi(n,m,t)_o \\ \psi(n,m,t)_i \end{pmatrix}. \tag{3.6}$$

As a result, a quantum walk on the Manhattan lattice which is homogeneous with respect to the cells can be viewed as a two-dimensional quantum walk on a Cartesian lattice driven by an 8 dimensional coin. The correspondence between the coordinates on the lattices is given as

$$(n,m) \longleftrightarrow \begin{aligned} 1&: (x,y) = (2n, 2m) \\ 2&: (x,y) = (2n+1, 2m) \\ 3&: (x,y) = (2n, 2m+1) \\ 4&: (x,y) = (2n+1, 2m+1) \end{aligned} \tag{3.7}$$

where the numbers 1,2,3,4 label the position in the cell (Figure 2).
The most general cell contains 4 different coins $C_1,\ C_2,\ C_3$ and C_4 at its 4 nodes. The action of these coins (3.2) on the coin space then reads

$$C_1 : (a_1 |U\rangle_i + b_1 |L\rangle_o) \langle U|_o + (c_1 |U\rangle_i + d_1 |L\rangle_o) \langle L|_i \tag{3.8}$$
$$C_2 : (a_2 |L\rangle_i + b_2 |D\rangle_o) \langle L|_o + (c_2 |L\rangle_i + d_2 |D\rangle_o) \langle D|_i \tag{3.9}$$
$$C_3 : (a_3 |R\rangle_i + b_3 |U\rangle_o) \langle R|_o + (c_3 |R\rangle_i + d_3 |U\rangle_o) \langle U|_i \tag{3.10}$$
$$C_4 : (a_4 |D\rangle_i + b_4 |R\rangle_o) \langle D|_o + (c_4 |D\rangle_i + d_4 |R\rangle_o) \langle R|_i \,. \tag{3.11}$$

The form of the coin that acts on the state (3.6) in the basis $\{|R\rangle_o, |U\rangle_o, |L\rangle_o, |D\rangle_o, |R\rangle_i, |U\rangle_i, |L\rangle_i, |D\rangle_i\}$ is given as

$$C = \begin{pmatrix} 0 & 0 & 0 & b_4 & d_4 & 0 & 0 & 0 \\ b_3 & 0 & 0 & 0 & 0 & d_3 & 0 & 0 \\ 0 & b_1 & 0 & 0 & 0 & 0 & d_1 & 0 \\ 0 & 0 & b_2 & 0 & 0 & 0 & 0 & d_2 \\ a_3 & 0 & 0 & 0 & 0 & c_3 & 0 & 0 \\ 0 & a_1 & 0 & 0 & 0 & 0 & c_1 & 0 \\ 0 & 0 & a_2 & 0 & 0 & 0 & 0 & c_2 \\ 0 & 0 & 0 & a_4 & c_4 & 0 & 0 & 0 \end{pmatrix}. \tag{3.12}$$

and its unitarity is equivalent to the unitarity of matrices (3.3) which represent unitary transformations at the nodes of the Manhattan lattice.
We see that a quantum walk on the Manhattan lattice can be represented by a quantum walk on two-dimensional Cartesian lattice driven by coin (3.12) with the conditional step operator given as

$$\begin{aligned} S = \sum_{n,m} \Big(& \Big(|L\rangle_i \langle L|_i + |D\rangle_i \langle D|_i + |U\rangle_i \langle U|_i + |R\rangle_i \langle R|_i \Big) \otimes |n,m\rangle \langle n,m| + |D\rangle_o \langle D|_o \otimes |n,m-1\rangle \langle n,m| \\ & + |U\rangle_o \langle U|_o \otimes |n,m+1\rangle \langle n,m| + |L\rangle_o \langle L|_o \otimes |n-1,m\rangle \langle n,m| + |R\rangle_o \langle R|_o \otimes |n+1,m\rangle \langle n,m| \Big). \end{aligned} \tag{3.13}$$

In the following we make a use of the correspondence between the quantum walk on the Manhattan lattice and the 8-state quantum walk on the Cartesian lattice to derive some of the interesting properties of the Manhattan walks.

3.1 Time evolution

Let us now focus on the time evolution of the 8-state quantum walk described above. One step is given as

$$\psi(n,m,t+1) = M_1\,\psi(n-1,m,t) + M_2\,\psi(n,m-1,t) + M_3\,\psi(n+1,m,t) + M_4\,\psi(n,m+1,t) + M_5\,\psi(n,m,t) \tag{3.14}$$

where $M_j,\ j \in \{1,2,3,4\}$ are matrices defined analogously to the matrices C^j (1.10) and correspond to the propagating part of the walk. M_5 is written as

$$M_5 = \begin{pmatrix} 0 & 0 & 0 & 0 & 0 & 0 & 0 & 0 \\ 0 & 0 & 0 & 0 & 0 & 0 & 0 & 0 \\ 0 & 0 & 0 & 0 & 0 & 0 & 0 & 0 \\ 0 & 0 & 0 & 0 & 0 & 0 & 0 & 0 \\ a_3 & 0 & 0 & 0 & 0 & c_3 & 0 & 0 \\ 0 & a_1 & 0 & 0 & 0 & 0 & c_1 & 0 \\ 0 & 0 & a_2 & 0 & 0 & 0 & 0 & c_2 \\ 0 & 0 & 0 & a_4 & c_4 & 0 & 0 & 0 \end{pmatrix} \tag{3.15}$$

and is associated with the motion inside the cell.
The Discrete-Time Fourier Transform (1.12) then yields the time evolution in the Fourier domain as

$$\tilde{\psi}(k,l,t) = \tilde{U}^t(k,l)\,\tilde{\psi}(k,l,0) \tag{3.16}$$

with the transformed evolution operator

$$\tilde{U}(k,l) = \mathrm{diag}\left(\mathrm{e}^{\mathrm{i}k}, \mathrm{e}^{\mathrm{i}l}, \mathrm{e}^{-\mathrm{i}k}, \mathrm{e}^{-\mathrm{i}l}, 1, 1, 1, 1\right) C. \tag{3.17}$$

In the analysis of quantum walks we are interested in the eigensystem of the evolution operator (3.17) from which we infer the dynamics of the quantum walk. Let us now analyse the spectrum of such an operator. The characteristic equation for the evolution operator (3.17) reads

$$\begin{aligned} \det\left(\tilde{U}(k,l) - \lambda\mathbb{I}\right) = \lambda^8 &+ \left(A_1\mathrm{e}^{\mathrm{i}k} + A_2\mathrm{e}^{-\mathrm{i}k} + A_3\mathrm{e}^{\mathrm{i}l} + A_4\mathrm{e}^{-\mathrm{i}l}\right)\lambda^6 \\ &+ \left(B + C_1\mathrm{e}^{\mathrm{i}(k+l)} + C_2e^{\mathrm{i}(k-l)} + C_3\mathrm{e}^{\mathrm{i}(-k+l)} + C_4\mathrm{e}^{\mathrm{i}(-k-l)}\right)\lambda^4 \\ &+ \left(D_1\mathrm{e}^{\mathrm{i}k} + D_2\mathrm{e}^{-\mathrm{i}k} + D_3\mathrm{e}^{\mathrm{i}l} + D_4\mathrm{e}^{-\mathrm{i}l}\right)\lambda^2 + \det C = 0, \end{aligned} \tag{3.18}$$

and $A_j,\ B,\ C_j$ and D_j are constants. It is easily seen that eigenvalues always come in pairs. Moreover, the degree of the polynomial in the characteristic equation (3.18) can be reduced to four when we substitute $\lambda^2 = \tilde{\lambda}$.
The characteristic equation can be readily separated in the following manner

$$\begin{aligned} \lambda^8 + B\lambda^4 + \det C = 0 \\ \left(C_1\mathrm{e}^{\mathrm{i}(k+l)} + C_2\mathrm{e}^{\mathrm{i}(k-l)} + C_3\mathrm{e}^{\mathrm{i}(-k+l)} + C_4\mathrm{e}^{\mathrm{i}(-k-l)}\right)\lambda^4 = 0 \\ \left(A_1\mathrm{e}^{\mathrm{i}k} + A_2\mathrm{e}^{-\mathrm{i}k} + A_3\mathrm{e}^{\mathrm{i}l} + A_4\mathrm{e}^{-\mathrm{i}l}\right)\lambda^6 + \left(D_1\mathrm{e}^{\mathrm{i}k} + D_2\mathrm{e}^{-\mathrm{i}k} + D_3\mathrm{e}^{\mathrm{i}l} + D_4\mathrm{e}^{-\mathrm{i}l}\right)\lambda^2 = 0. \end{aligned} \tag{3.19}$$

The first of the relations (3.19) is obtained when we substitute in (3.18) $(k,l) = (0,0),\ (k,l) = (0,\pi),\ (k,l) = (\pi,0)$ and $(k,l) = (\pi,\pi)$ consecutively and add the relations. Similarly, the third one is separated using substitutions $(k,l) = (k,0),\ (k,l) = (k,\pi),\ (k,l) = (0,l)$ and $(k,l) = (\pi,l)$. One can immediately see from relations (3.19) that λ being a constant eigenvalue of the step operator (3.17) imply that $-\lambda$ and $\pm\mathrm{i}\lambda$ also belong to the spectrum of this operator.

3.2 Trapping effect in quantum walks on the Manhattan lattice

In the following we analyse under which conditions the quantum walks described above exhibit the trapping effect by imposing conditions on the spectrum of the matrix $\tilde{U}(k,l)$. We consider the most general case when the quantum walk has 4 different coins at each node in a cell.

The characteristic equation for the general constant eigenvalue $e^{i\varphi},\ \varphi \in \mathbb{R}$ reads

$$\det\left(\tilde{U}(k,l) - \mathrm{e}^{\mathrm{i}\varphi}\mathbb{I}\right) = 0 \tag{3.20}$$

and takes the form of (3.18). Since this equation holds for arbitrary k, l we obtain following relations for the coin parameters $a_i,\ b_i,\ c_i,\ d_i,\ i \in \{1,2,3,4\}$ using similar reasoning as in the case of the relations (3.19)

$$\begin{aligned}
\mathrm{e}^{\mathrm{i}l}: &\quad -a_1d_3\mathrm{e}^{6\mathrm{i}\varphi} - a_2b_1b_3c_1c_3d_4\mathrm{e}^{2\mathrm{i}\varphi} + a_1a_2b_3c_3d_1d_4\mathrm{e}^{2\mathrm{i}\varphi} + a_2a_3b_1c_1d_3d_4\mathrm{e}^{2\mathrm{i}\varphi} - a_1a_2a_3d_1d_3d_4\mathrm{e}^{2\mathrm{i}\varphi} = 0\\
\mathrm{e}^{-\mathrm{i}l}: &\quad -a_4d_2\mathrm{e}^{6\mathrm{i}\varphi} - a_3b_2b_4c_2c_4d_1\mathrm{e}^{2\mathrm{i}\varphi} + a_2a_3b_4c_4d_1d_2\mathrm{e}^{2\mathrm{i}\varphi} + a_3a_4b_2c_2d_1d_4\mathrm{e}^{2\mathrm{i}\varphi} - a_2a_3a_4d_1d_2d_4\mathrm{e}^{2\mathrm{i}\varphi} = 0\\
\mathrm{e}^{\mathrm{i}k}: &\quad -a_3d_4\mathrm{e}^{6\mathrm{i}\varphi} - a_1a_3a_4d_2d_3d_4\mathrm{e}^{2\mathrm{i}\varphi} + a_1a_4b_3c_3d_2d_4\mathrm{e}^{2\mathrm{i}\varphi} + a_1a_3b_4c_4d_2d_3\mathrm{e}^{2\mathrm{i}\varphi} - a_1b_3b_4c_3c_4d_2\mathrm{e}^{2\mathrm{i}\varphi} = 0\\
\mathrm{e}^{-\mathrm{i}k}: &\quad -a_2d_1\mathrm{e}^{6\mathrm{i}\varphi} - a_4b_1b_2c_1c_2d_3\mathrm{e}^{2\mathrm{i}\varphi} + a_1a_4b_2c_2d_1d_3\mathrm{e}^{2\mathrm{i}\varphi} + a_2a_4b_1c_1d_2d_3\mathrm{e}^{2\mathrm{i}\varphi} - a_1a_2a_4d_1d_2d_3\mathrm{e}^{2\mathrm{i}\varphi} = 0
\end{aligned} \tag{3.21}$$

$$\begin{aligned}
\mathrm{e}^{\mathrm{i}(k+l)}: &\quad a_1a_3d_3d_4\mathrm{e}^{4\mathrm{i}\varphi} - a_1b_3c_3d_4\mathrm{e}^{4\mathrm{i}\varphi} = 0\\
\mathrm{e}^{\mathrm{i}(k-l)}: &\quad a_3a_4d_2d_4\mathrm{e}^{4\mathrm{i}\varphi} - a_3b_4c_4d_2\mathrm{e}^{4\mathrm{i}\varphi} = 0\\
\mathrm{e}^{\mathrm{i}(-k+l)}: &\quad a_1a_2d_1d_3\mathrm{e}^{4\mathrm{i}\varphi} - a_2b_1c_1d_3\mathrm{e}^{4\mathrm{i}\varphi} = 0\\
\mathrm{e}^{\mathrm{i}(-k-l)}: &\quad a_2a_4d_1d_2\mathrm{e}^{4\mathrm{i}\varphi} - a_4b_2c_2d_1\mathrm{e}^{4\mathrm{i}\varphi} = 0
\end{aligned} \tag{3.22}$$

$$\begin{aligned}
&\mathrm{e}^{8\mathrm{i}\varphi} - b_1b_2b_3b_4\mathrm{e}^{4\mathrm{i}\varphi} + a_1a_4d_2d_3\mathrm{e}^{4\mathrm{i}\varphi} + a_2a_3d_1d_4\mathrm{e}^{4\mathrm{i}\varphi} - c_1c_2c_3c_4\mathrm{e}^{4\mathrm{i}\varphi} + a_1a_2a_3a_4d_1d_2d_3d_4\\
&- a_1a_2a_3b_4c_4d_1d_2d_3 - a_1a_2a_4b_3c_3d_1d_2d_4 + a_1a_2b_3b_4c_3c_4d_1d_2 - a_1a_3a_4b_2c_2d_1d_3d_4 + a_1a_3b_2b_4c_2c_4d_1d_3\\
&+ a_1a_4b_2b_3c_2c_3d_1d_4 - a_1b_2b_3b_4c_2c_3c_4d_1 - a_2a_3a_4b_1c_1d_2d_3d_4 + a_2a_3b_1b_4c_1c_4d_2d_3 + a_2a_4b_1b_3c_1c_3d_2d_4\\
&-a_2b_1b_3b_4c_1c_3c_4d_2+a_3a_4b_1b_2c_1c_2d_3d_4-a_3b_1b_2b_4c_1c_2c_4d_3-a_4b_1b_2b_3c_1c_2c_3d_4+b_1b_2b_3b_4c_1c_2c_3c_4 = 0
\end{aligned} \tag{3.23}$$

Relations (3.22) imply

$$a_1d_4 = 0 \quad a_2d_3 = 0 \quad a_3d_2 = 0 \quad a_4d_1 = 0 \tag{3.24}$$

since the determinant of the unitary matrices (3.3) is never equal to zero. These conditions together with conditions (3.21) yield the solution in the form of

$$C_i = \begin{pmatrix} 0 & c_i \\ b_i & 0 \end{pmatrix}, \quad C_j = \begin{pmatrix} 0 & c_j \\ b_j & 0 \end{pmatrix}, \quad C_k = \begin{pmatrix} 0 & c_k \\ b_k & 0 \end{pmatrix}, \quad C_l = \begin{pmatrix} a_l & c_l \\ b_l & d_l \end{pmatrix}, \tag{3.25}$$

where i, j, k, l are pair-wise distinct indexes from $\{1,2,3,4\}$. The equation (3.23) then puts another restriction on the on the matrices (3.25) in the form of

$$\mathrm{e}^{8\mathrm{i}\varphi} - b_ib_jb_kb_l\mathrm{e}^{4\mathrm{i}\varphi} - c_ic_jc_kc_l\mathrm{e}^{4\mathrm{i}\varphi} - b_ib_jb_kc_ic_jc_k(a_ld_l - b_lc_l) = 0 \tag{3.26}$$

Let us now assume without a loss of generality that the index l in (3.25) is equal to 4. The characteristic equation for the solution given by (3.25) attains a simple form

$$\lambda^8 - (b_1b_2b_3b_4 + c_1c_2c_3c_4)\lambda^4 - b_1b_2b_3c_1c_2c_3(a_4d_4 - b_4c_4) = 0. \tag{3.27}$$

and does not depend on k, l. As a consequence, the trapping effect in case of quantum walks driven by the coin (3.12) is trivial since the evolution operator $\tilde{U}(k,l)$ possess only the point spectrum.

At this point we restrict ourselves to solutions of (3.26) in the form of SU(2). An arbitrary SU(2) matrix can be parametrized as

$$M = \begin{pmatrix} |a|\mathrm{e}^{\mathrm{i}\alpha} & |b|\mathrm{e}^{\mathrm{i}\beta} \\ -|b|\mathrm{e}^{-\mathrm{i}\beta} & |a|\mathrm{e}^{-\mathrm{i}\alpha} \end{pmatrix}, \quad |a|^2 + |b|^2 = 1, \quad |a|, |b|, \alpha, \beta \in \mathbb{R}. \tag{3.28}$$

Using this parametrization for matrices (3.25) we obtain the general SU(2) solution of (3.26) dependent on 6 real parameters as

$$C_i = \begin{pmatrix} 0 & \mathrm{e}^{\mathrm{i}\alpha_i} \\ -\mathrm{e}^{-\mathrm{i}\alpha_i} & 0 \end{pmatrix}, \ i \in \{1,2,3\}, \quad C_{4\pm} = \begin{pmatrix} \pm\sqrt{1 - \frac{\cos^2(4\varphi)}{\cos^2(\alpha_1+\alpha_2+\alpha_3+\beta)}}\mathrm{e}^{\mathrm{i}\alpha} & \frac{\cos(4\varphi)}{\cos(\alpha_1+\alpha_2+\alpha_3+\beta)}e^{\mathrm{i}\beta} \\ -\frac{\cos(4\varphi)}{\cos(\alpha_1+\alpha_2+\alpha_3+\beta)}e^{-\mathrm{i}\beta} & \pm\sqrt{1 - \frac{\cos^2(4\varphi)}{\cos^2(\alpha_1+\alpha_2+\alpha_3+\beta)}}\mathrm{e}^{-\mathrm{i}\alpha} \end{pmatrix}. \tag{3.29}$$

Let us now turn to the analysis of the trapping coins derived above. The characteristic equation for the evolution operator $\tilde{U}(k,l)$ corresponding to the trapping 8-state coin (3.12) using the above SU(2) solution (3.29) is obtained as

$$\lambda^8 - 2\cos(4\varphi)\lambda^4 + 1 = 0. \tag{3.30}$$

The eigenvalues take the following form for both coins $C_{4\pm}$

$$\lambda_{1,2} = \pm\mathrm{e}^{\mathrm{i}\varphi}, \quad \lambda_{3,4} = \pm\mathrm{e}^{-\mathrm{i}\varphi}, \quad \lambda_{5,6} = \pm\mathrm{i}\mathrm{e}^{\mathrm{i}\varphi}, \quad \lambda_{7,8} = \pm\mathrm{i}\mathrm{e}^{-\mathrm{i}\varphi} \tag{3.31}$$

and the corresponding eigenvalues for the coin C_{4+} read

$$v_{1,2}(k,l) = \frac{1}{2\sqrt{\mu^2+\nu_+^2}} \begin{pmatrix} \mu\,\mathrm{e}^{\mathrm{i}k}\mathrm{e}^{-\mathrm{i}(\alpha-\alpha_1-\alpha_2-\alpha_3-4\varphi)} \\ \mp\mu\,\mathrm{e}^{\mathrm{i}(k+l)}\mathrm{e}^{-\mathrm{i}(\alpha-\alpha_1-\alpha_2-3\varphi)} \\ \mu\,\mathrm{e}^{\mathrm{i}l}\mathrm{e}^{-\mathrm{i}(\alpha-\alpha_2-2\varphi)} \\ \mp\mu\,\mathrm{e}^{-\mathrm{i}(\alpha-\varphi)} \\ \pm\nu_+\,\mathrm{e}^{\mathrm{i}(\alpha_1+\alpha_2+\alpha_3-3\varphi)} \\ \nu_+\,\mathrm{e}^{\mathrm{i}(\alpha_1+\alpha_2-2\varphi)} \\ \pm\nu_+\,\mathrm{e}^{\mathrm{i}(\alpha_2-\varphi)} \\ \nu_+ \end{pmatrix} \quad v_{3,4}(k,l) = \frac{1}{2\sqrt{\mu^2+\nu_-^2}} \begin{pmatrix} \mu\,\mathrm{e}^{\mathrm{i}k}\mathrm{e}^{-\mathrm{i}(\alpha-\alpha_1-\alpha_2-\alpha_3+4\varphi)} \\ \mp\mu\,\mathrm{e}^{\mathrm{i}(k+l)}\mathrm{e}^{-\mathrm{i}(\alpha-\alpha_1-\alpha_2+3\varphi)} \\ \mu\,\mathrm{e}^{\mathrm{i}l}\mathrm{e}^{-\mathrm{i}(\alpha-\alpha_2+2\varphi)} \\ \mp\mu\,\mathrm{e}^{-\mathrm{i}(\alpha+\varphi)} \\ \pm\nu_-\,\mathrm{e}^{\mathrm{i}(\alpha_1+\alpha_2+\alpha_3+3\varphi)} \\ \nu_-\,\mathrm{e}^{\mathrm{i}(\alpha_1+\alpha_2+2\varphi)} \\ \pm\nu_-\,\mathrm{e}^{\mathrm{i}(\alpha_2+\varphi)} \\ \nu_- \end{pmatrix}$$

$$v_{5,6}(k,l) = \frac{1}{2\sqrt{\mu^2+\nu_+^2}} \begin{pmatrix} \mu\,\mathrm{e}^{\mathrm{i}k}\mathrm{e}^{-\mathrm{i}(\alpha-\alpha_1-\alpha_2-\alpha_3-4\varphi)} \\ \pm\mathrm{i}\,\mu\,\mathrm{e}^{\mathrm{i}(k+l)}\mathrm{e}^{-\mathrm{i}(\alpha-\alpha_1-\alpha_2-3\varphi)} \\ -\mu\,\mathrm{e}^{\mathrm{i}l}\mathrm{e}^{-\mathrm{i}(\alpha-\alpha_2-2\varphi)} \\ \mp\mathrm{i}\,\mu\,\mathrm{e}^{-\mathrm{i}(\alpha-\varphi)} \\ \pm\mathrm{i}\,\nu_+\,\mathrm{e}^{\mathrm{i}(\alpha_1+\alpha_2+\alpha_3-3\varphi)} \\ -\nu_+\,\mathrm{e}^{\mathrm{i}(\alpha_1+\alpha_2-2\varphi)} \\ \mp\mathrm{i}\,\nu_+\,\mathrm{e}^{\mathrm{i}(\alpha_2-\varphi)} \\ \nu_+ \end{pmatrix} \quad v_{7,8}(k,l) = \frac{1}{2\sqrt{\mu^2+\nu_-^2}} \begin{pmatrix} \mu\,\mathrm{e}^{\mathrm{i}k}\mathrm{e}^{-\mathrm{i}(\alpha-\alpha_1-\alpha_2-\alpha_3+4\varphi)} \\ \pm\mathrm{i}\,\mu\,\mathrm{e}^{\mathrm{i}(k+l)}\mathrm{e}^{-\mathrm{i}(\alpha-\alpha_1-\alpha_2+3\varphi)} \\ -\mu\,\mathrm{e}^{\mathrm{i}l}\mathrm{e}^{-\mathrm{i}(\alpha-\alpha_2+2\varphi)} \\ \mp\mathrm{i}\,\mu\,\mathrm{e}^{-\mathrm{i}(\alpha+\varphi)} \\ \pm\mathrm{i}\,\nu_-\,\mathrm{e}^{\mathrm{i}(\alpha_1+\alpha_2+\alpha_3+3\varphi)} \\ -\nu_-\,\mathrm{e}^{\mathrm{i}(\alpha_1+\alpha_2+2\varphi)} \\ \mp\mathrm{i}\,\nu_-\,\mathrm{e}^{\mathrm{i}(\alpha_2+\varphi)} \\ \nu_- \end{pmatrix}$$

where we have used the abbreviations

$$\mu = \sqrt{\mathrm{e}^{4\mathrm{i}(\alpha_1+\alpha_2+\alpha_3+\beta)} - 2\cos(8\varphi)\,\mathrm{e}^{2\mathrm{i}(\alpha_1+\alpha_2+\alpha_3+\beta)} + 1} \tag{3.32}$$

$$\nu_\pm = \mathrm{e}^{2\mathrm{i}(\alpha_1+\alpha_2+\alpha_3+\beta)}\mathrm{e}^{\pm 8\mathrm{i}\varphi} - 1. \tag{3.33}$$

The eigenvectors $\tilde{v}_j$ in case of the C_{4-} coin take similar form given by

$$\tilde{v_j} = \mathrm{diag}(-1,-1,-1,-1,1,1,1,1)\,v_j, \quad j \in \{1,2,3,4,5,6,7,8\}. \tag{3.34}$$

Application of the inverse Fourier Transform yields that the support of the eigenvectors is finite and the form of the stationary states in the Cartesian coordinates (n,m) and the coordinates (x,y) on the Manhattan lattice, respectively, reads

$$\begin{aligned} v_j(n,m) = a_j\,|R\rangle_o \otimes |n+1,m\rangle + b_j\,|U\rangle_o \otimes |n+1,m+1\rangle + c_j\,|L\rangle_o \otimes |n,m+1\rangle \\ + \left(d_j\,|D\rangle_o + e_j\,|R\rangle_i + f_j\,|U\rangle_i + g_j\,|L\rangle_i + h_j\,|D\rangle_i\right) \otimes |n,m\rangle \end{aligned} \tag{3.35}$$

$$\begin{aligned} v_j(x,y) = a_j\,|R\rangle_o \otimes |x+2,y+1\rangle + b_j\,|U\rangle_o \otimes |x+2,y+2\rangle + c_j\,|L\rangle_o \otimes |x+1,y+2\rangle \\ + d_j\,|D\rangle_o \otimes |x+1,y+1\rangle + e_j\,|R\rangle_i \otimes |x+1,y+1\rangle \\ + f_j\,|U\rangle_i \otimes |x,y+1\rangle + g_j\,|L\rangle_i \otimes |x,y\rangle + h_j\,|D\rangle_i \otimes |x+1,y\rangle \end{aligned} \tag{3.36}$$

where $a_j,\ b_j,\ c_j,\ d_j,\ e_j,\ f_j,\ g_j$ and h_j are constants for $j \in \{1,2,3,4,5,6,7,8\}$.

We conclude that the trapping effect in case a of homogeneous quantum walk on the Manhattan lattice is trivial since the trapping coins possess only the point spectrum.

3.3 Quantum walk on the Manhattan lattice with the Hadamard coin

In this section we consider quantum walks on the Manhattan lattice driven by the well-studied Hadamard coin

$$H = \frac{1}{\sqrt{2}}\begin{pmatrix} 1 & 1 \\ 1 & -1 \end{pmatrix}. \tag{3.37}$$

This quantum walk corresponds to 8-state quantum walk on a two-dimensional Cartesian lattice with the coin C_H in the form of (3.12) written as

$$C_H = \begin{pmatrix} 0 & 0 & 0 & \frac{1}{\sqrt{2}} & -\frac{1}{\sqrt{2}} & 0 & 0 & 0 \\ \frac{1}{\sqrt{2}} & 0 & 0 & 0 & 0 & -\frac{1}{\sqrt{2}} & 0 & 0 \\ 0 & \frac{1}{\sqrt{2}} & 0 & 0 & 0 & 0 & -\frac{1}{\sqrt{2}} & 0 \\ 0 & 0 & \frac{1}{\sqrt{2}} & 0 & 0 & 0 & 0 & -\frac{1}{\sqrt{2}} \\ \frac{1}{\sqrt{2}} & 0 & 0 & 0 & 0 & \frac{1}{\sqrt{2}} & 0 & 0 \\ 0 & \frac{1}{\sqrt{2}} & 0 & 0 & 0 & 0 & \frac{1}{\sqrt{2}} & 0 \\ 0 & 0 & \frac{1}{\sqrt{2}} & 0 & 0 & 0 & 0 & \frac{1}{\sqrt{2}} \\ 0 & 0 & 0 & \frac{1}{\sqrt{2}} & \frac{1}{\sqrt{2}} & 0 & 0 & 0 \end{pmatrix}. \tag{3.38}$$

The eigenvalues of the step operator in the Fourier Domain $\tilde{U}_H(k,l)$ are obtained as

$$\lambda_{1,2} = \pm\frac{1}{2}\left(-\cos k - \cos l + \kappa + \sqrt{2\cos^2 k - 4\cos k\cos l + 2\cos^2 l - (2\cos k + 2\cos l)\kappa - 8}\right)^{1/2}$$
$$\lambda_{3,4} = \pm\frac{1}{2}\left(-\cos k - \cos l + \kappa - \sqrt{2\cos^2 k - 4\cos k\cos l + 2\cos^2 l - (2\cos k + 2\cos l)\kappa - 8}\right)^{1/2}$$
$$\lambda_{5,6} = \pm\frac{1}{2}\left(-\cos k - \cos l - \kappa + \sqrt{2\cos^2 k - 4\cos k\cos l + 2\cos^2 l + (2\cos k + 2\cos l)\kappa - 8}\right)^{1/2}$$
$$\lambda_{7,8} = \pm\frac{1}{2}\left(-\cos k - \cos l - \kappa - \sqrt{2\cos^2 k - 4\cos k\cos l + 2\cos^2 l + (2\cos k + 2\cos l)\kappa - 8}\right)^{1/2}$$

and we have used the abbreviation

$$\kappa = \sqrt{\cos^2 k - 6\cos k\cos l + \cos^2 l + 8}. \tag{3.39}$$

It can be proven that the following inequality

$$2\cos^2 k - 4\cos k\cos l + 2\cos^2 l \pm (2\cos k + 2\cos l)\kappa - 8 \tag{3.40}$$

holds for every k, l. As a result, the eigenvalues can be obtained in the following form

$$\lambda_{1,2} = \pm e^{\frac{i\omega_1(k,l)}{2}}, \quad \cos(\omega_{1,2}(k,l)) = \frac{1}{4}\left(-\cos k - \cos l \pm \sqrt{\cos^2 k - 6\cos k\cos l + \cos^2 l + 8}\right)$$
$$\lambda_{3,4} = \pm e^{-\frac{i\omega_1(k,l)}{2}}$$
$$\lambda_{5,6} = \pm e^{\frac{i\omega_2(k,l)}{2}}, \quad \sin(\omega_{1,2}(k,l)) = -i\sqrt{2\cos^2 k - 4\cos k\cos l + 2\cos^2 l \pm (2\cos k + 2\cos l)\kappa - 8}$$
$$\lambda_{7,8} = \pm e^{\frac{i\omega_2(k,l)}{2}}.$$

The Figure 3.2 show the probability distribution for the Hadamard walk on the Manhattan lattice and the Hadamard walk driven by the 8-dimensional coin operator C_H on the Cartesian lattice, respectively, starting at the origin. It also illustrates the dependence of the probability distribution on the choice of the initial state for three different initial states (written with respect to the quantum walk on the Manhattan lattice and with respect to the 8-state quantum walk on the Cartesian lattice)

$$\begin{aligned} \psi_1 &= \frac{1}{\sqrt{2}}(0,1,i,0)^T & \psi_1 &= \frac{1}{\sqrt{2}}(0,1,0,0,0,0,i,0)^T \\ \psi_2 &= \frac{1}{\sqrt{2}}(0,1,1,0)^T \quad \longleftrightarrow & \psi_2 &= \frac{1}{\sqrt{2}}(0,1,0,0,0,0,1,0)^T \\ \psi_3 &= (0,0,1,0)^T & \psi_3 &= (0,0,0,0,0,0,1,0)^T \end{aligned} \tag{3.41}$$

As expected from the bijection (3.7), the quantum walk on the Manhattan lattice propagates two times faster than the corresponding 8-state quantum walk and the probability distributions exhibit the same positions of the peaks.

3.3.1 Pólya number

Let us now turn to the Pólya number for the Hadamard walk. The method of stationary phase used in [16] cannot be employed in this case since the partial derivatives of the function $\omega_2(k,l)$ is not defined for every $k \in (-\pi,\pi), l \in (-\pi,\pi)$.

Based on the simulation, we can formulate a hypothesis stating that the Hadamard walk is transient. Figure 3.3 depicts the time-dependence of the probability p_0 of being at the origin for three different initial states (3.41). The red curve showing the behaviour of p_0 decays as $t^{-1.95}$, $t^{-2.48}$ and $t^{-2.30}$, respectively, which suggests that the Pólya number is less than 1.

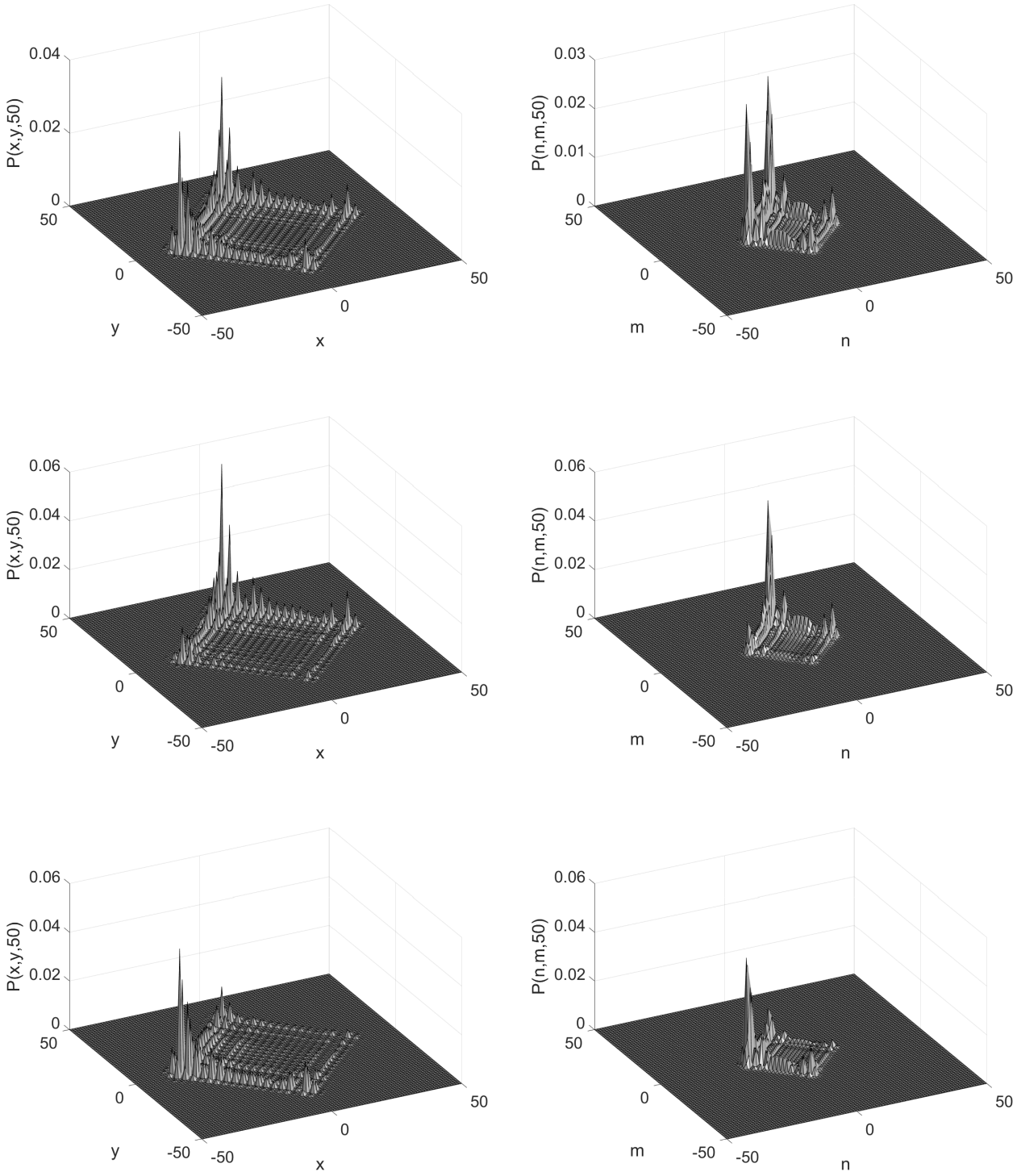

Figure 3.2: The probability distribution for the Hadamard walk with 3 different initial states given by (3.41) after 50 steps. The probability distribution with respect to the Manhattan lattice is depicted on the left, the corresponding probability distribution for the 8-state quantum walk on the Cartesian lattice is on the right. We see that the distribution in the former case propagates two times faster and the shape of the probability distribution is the same, as expected.

3.4 Quantum walk on the Manhattan lattice with the rotation coin

Another interesting example of two-dimensional coins is that of the rotation coin given as

$$R = \begin{pmatrix} \cos\theta & -\sin\theta \\ \sin\theta & \cos\theta \end{pmatrix}. \tag{3.42}$$

where we restrict ourselves to $\theta \in [0, \pi/2]$.
Similarly to the previous quantum walk with the Hadamard coin, we analyse the spectrum of the 8-dimensional coin $C_R(\theta)$ given by

$$C_R(\theta) = \begin{pmatrix} 0 & 0 & 0 & \sin\theta & \cos\theta & 0 & 0 & 0 \\ \sin\theta & 0 & 0 & 0 & 0 & \cos\theta & 0 & 0 \\ 0 & \sin\theta & 0 & 0 & 0 & 0 & \cos\theta & 0 \\ 0 & 0 & \sin\theta & 0 & 0 & 0 & 0 & \cos\theta \\ \cos\theta & 0 & 0 & 0 & 0 & -\sin\theta & 0 & 0 \\ 0 & \cos\theta & 0 & 0 & 0 & 0 & -\sin\theta & 0 \\ 0 & 0 & \cos\theta & 0 & 0 & 0 & 0 & -\sin\theta \\ 0 & 0 & 0 & \cos\theta & -\sin\theta & 0 & 0 & 0 \end{pmatrix}. \tag{3.43}$$

The characteristic polynomial of $\tilde{U}_R(\theta, k, l)$ reads

$$\lambda^8 - 2\lambda^6 \cos^2\theta\Big(\cos k + \cos l\Big) + 2\lambda^4\Big(2\cos^2\theta\cos k\cos l + 2\cos^2\theta - 1\Big) - 2\lambda^2\cos^2\theta\Big(\cos k + \cos l\Big) + 1 = 0. \tag{3.44}$$

The eigenvalues take similar form as those of the Hadamard walk

$$\lambda_{1,2} = \pm e^{\frac{i\omega_1(k,l)}{2}}, \quad \cos(\omega_{1,2}(k,l)) = \frac{1}{2}\left((\cos k + \cos l)\cos\theta \pm \kappa\right)$$
$$\lambda_{3,4} = \pm e^{-\frac{i\omega_1(k,l)}{2}}$$
$$\lambda_{5,6} = \pm e^{\frac{i\omega_2(k,l)}{2}}, \quad \sin(\omega_{1,2}(k,l)) = -i\frac{\sqrt{2}}{2}\sqrt{(\cos k + \cos l)\kappa + (\cos k + \cos l)^2\cos^2\theta - 2\cos k\cos l - 2}$$
$$\lambda_{7,8} = \pm e^{-\frac{i\omega_2(k,l)}{2}}$$

where

$$\kappa = \sqrt{(\cos k + \cos l)^2\cos^4\theta - 4(\cos k\cos l + 1)\cos^2\theta + 4} \tag{3.45}$$

At this point we note that the properties of the quantum walks driven by the rotation coin depend significantly on the coin parameter θ. From the above equations follows that the trapping effect is present only for $\theta = 0$; i.e. the dependence of the eigenvalues on k, l vanishes. On the contrary, a coin with θ set to $\pi/2$ results in a quantum walk propagating with the maximum velocity.
Note that these two examples correspond to the classical random walk on the Manhattan lattice in case of full presence/absence of the scatterers (the former adding a phase shift of π for the motion inside the cell).

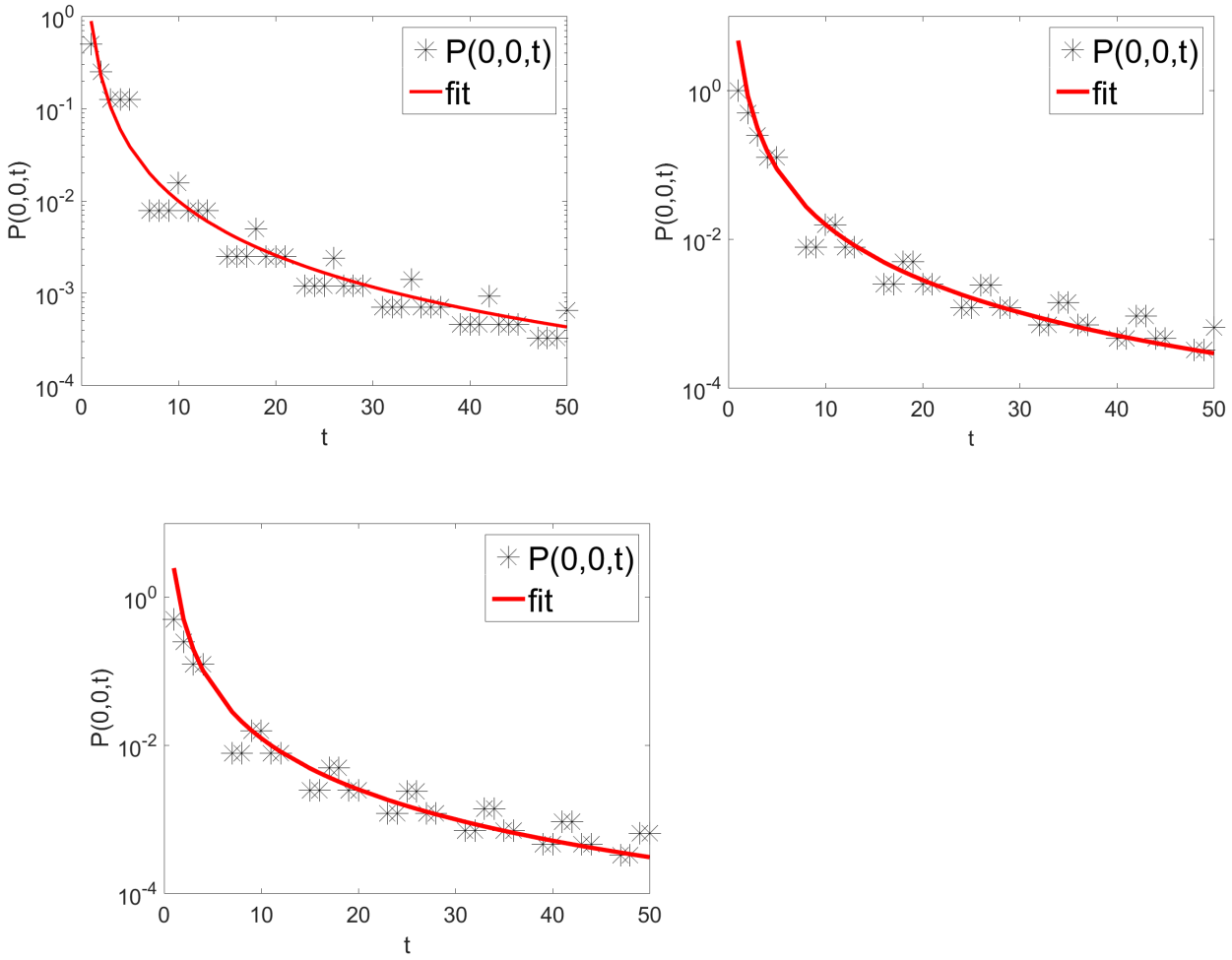

Figure 3.3: The probability $p_0(t)$ of being at the origin at time t for 3 different initial states ψ_1, ψ_2 and ψ_3 given by (3.41) in case of the 8-state Hadamard walk (semilog plot).

3.5 Quantum walks on the finite Manhattan lattice

Let us now focus on the homogeneous quantum walks on the finite Manhattan lattice. In this case the boundary conditions have to be taken into consideration. We deal only with absorbing and periodic boundaries; the reflecting boundary conditions cannot be employed as we have a lattice with directed edges.

3.5.1 Absorbing boundaries

Let us assume that we have finite $2N \times 2M$ Manhattan lattice with absorbing boundaries where N, M are even. The position space is given as a span $= \{|x, y\rangle \,|\, -N \leq x \leq N-1, -M \leq y \leq M-1\}$ and we assume the boundary to be described by lines $x = -N,\ x = N-1,\ y = -M$ and $y = M-1$.
As we have already discussed in the previous chapter, quantum walk on this Manhattan lattice can be viewed as 8-state quantum walk on the $(N+1) \times (M+1)$ Cartesian lattice. The position space on this lattice has this form span$\{|n, m\rangle \,|\, -N/2 \leq n \leq N/2, -M/2 \leq m \leq M/2\}$ due to the correspondence (3.7).

One step of a quantum walk has the form of (1.2) where S is the shift operator (3.13) and the coin C corresponds to the Hadamard coin (3.38).
To employ absorbing boundaries we apply projection Π at each step (see [17]) on the position space

$$\Pi = \mathbb{I} - \sum_{j=-N/2}^{N/2} \sum_{k=-M/2}^{M/2} \Big(|j, -M/2\rangle\otimes\langle j, -M/2| + |j, M/2\rangle\otimes\langle j, M/2| + |-N/2, k\rangle\otimes\langle -N/2, k| + |N/2, k\rangle\otimes\langle N/2, k| \Big) \tag{3.46}$$

and one step of the quantum walk then takes this form

$$U_{abs} = (\mathbb{I}_c \otimes \Pi)\, U \tag{3.47}$$

i.e. the probability amplitude arriving at the boundary does not affect the further evolution. As a result, the time evolution is no longer unitary and the absolute value of the eigenvalues corresponding to the evolution operator U_{abs} is less than one (except for special cases when the quantum walk is trapped at the origin).
The survival probability is given as

$$P(t) = |\psi(t)|^2 \tag{3.48}$$

$$= |(\Pi\, U)^t \psi(0)|^2 \tag{3.49}$$

and its asymptotic behaviour can be estimated as

$$P(t) \sim \mathrm{e}^{-\gamma t}, \quad \gamma = 2(1 - |\lambda|) \tag{3.50}$$

where λ is the largest eigenvalue in the absolute value (for details see [17]).

The table (3.5.1) shows the largest eigenvalues in the absolute value of the operator U_{abs} obtained numerically for the 8-state quantum walks driven by the Hadamard coin C_R and the rotation coin $C_R(\theta)$. We have considered square Cartesian lattices of the size 5×5 ($N/2 = 2$), 7×7 ($N/2 = 3$) , 9×9 ($N/2 = 4$) and 11×11 ($N/2 = 5$). We see that with the growing size of the square lattice the largest eigenvalue in the absolute value is closer to 1. In other words, the survival probability decays slower, as was expected. Moreover, both of the quantum walks driven by the balanced coins C_H and $C_R(\pi/4)$ exhibit the same asymptotic behaviour of the discussed probability. Notice also that the decay of the survival probability is slower in the case of unbalanced coin $C_R(\pi/3)$.

$N/2$	C_H	$C_R\left(\frac{\pi}{4}\right)$	$C_R\left(\frac{\pi}{3}\right)$
2	0.96174062820	0.96174062820	0.98599280634
3	0.98947270362	0.98947270362	0.99648848064
4	0.99584144653	0.99584144653	0.99866156908
5	0.99797259408	0.99797259408	0.99935818345

Table 3.1: The largest eigenvalues in the absolute value of the operator U_{abs} for the Hadamard walk and for the quantum walk with the rotation coin for $\theta = \frac{\pi}{4}, \theta = \frac{\pi}{3}$.

Figures 3.4 and 3.5 show the probability distribution for quantum walk starting at the origin with the initial state $\psi_{in} = \frac{1}{\sqrt{2}}(0, 1, \mathrm{i}, 0)$ in case of 40×40 Manhattan lattice and in case of the equivalent quantum walk on the Cartesian lattice with the same initial state corresponding to $\psi_{in} = \frac{1}{\sqrt{2}}(0, 1, 0, 0, 0, 0, \mathrm{i}, 0)$. We see that with increasing number of steps the propagating peaks die out, the probability distribution

looses its characteristic shape and starts to look randomly. This behaviour stems from the fact that the evolution is no longer unitary as the effect of decoherence occurs at the boundary.
Figure 3.6 then shows how the overall probability of finding the walker on the lattice evolves in time for three different initial states (3.41). We see that our choice of the initial state does not significantly affect the discussed probability.
Figure 3.7 depicts the survival probability in case of the 9×9 Cartesian lattice for the Hadamard walk and for the quantum walk with the rotation coin $C_R(\pi/3)$ on a log scale. We see that for large times t the survival probability corresponds well with the estimate given by (3.50), i. e. the survival probability decays exponentially. Note that the survival probability decays faster in the case of the rotation coin, as we expected.

3.5.2 Periodic boundaries

In this section we consider the same square $(N+1)\times(N+1)$ Cartesian lattice described above. However, we employ the periodic boundary conditions identifying position $-N$ with N which is equivalent to the square lattice distorted into the shape of a torus.
The time evolution of the 8-state quantum walk on this lattice can be obtained by the Fourier Transform (for detailed computation see [18]) and is given as

$$\tilde{U}(k,l) = \mathrm{diag}\,(\omega^k, \omega^l, \omega^{-k}, \omega^{-l}, 1, 1, 1, 1)\, C. \tag{3.51}$$

where $\omega = \mathrm{e}^{\frac{2i\pi}{N}}$ and $k, l \in \{0, 1, \ldots, N-1\}$.
Having described a method how to obtain the spectrum of a homogeneous quantum walk easily, we can apply it to compute the spectrum of the classical random walks on the Manhattan lattice with periodic boundaries in case of full presence and full absence of the scatterers.
The corresponding coins C_0 and C_1 for the probability of the scatterers $p = 0$ and $p = 1$ take the form of

$$C_0 = \begin{pmatrix} 0&0&0&0&1&0&0&0\\ 0&0&0&0&0&1&0&0\\ 0&0&0&0&0&0&1&0\\ 0&0&0&0&0&0&0&1\\ 1&0&0&0&0&0&0&0\\ 0&1&0&0&0&0&0&0\\ 0&0&1&0&0&0&0&0\\ 0&0&0&1&0&0&0&0 \end{pmatrix} \qquad C_1 = \begin{pmatrix} 0&0&0&1&0&0&0&0\\ 1&0&0&0&0&0&0&0\\ 0&1&0&0&0&0&0&0\\ 0&0&1&0&0&0&0&0\\ 0&0&0&0&0&1&0&0\\ 0&0&0&0&0&0&1&0\\ 0&0&0&0&0&0&0&1\\ 0&0&0&0&1&0&0&0 \end{pmatrix}. \tag{3.52}$$

The Fourier Transform leads us to the spectrum of the evolution operators in the Fourier domain given by

$$\lambda_0 = \{\pm\mathrm{e}^{\pm\frac{ik}{N}}, \pm\mathrm{e}^{\pm\frac{il}{N}}\} \tag{3.53}$$

$$\lambda_1 = \{\pm 1, \pm\mathrm{i}\}. \tag{3.54}$$

In the case of the coin C_1 we have obtained double degenerate constant eigenvalues that indicate the presence of the trapping effect, as expected.

Another interesting example of homogeneous quantum walk on the Manhattan lattice is that with two non-interacting one-dimensional quantum walks moving in the opposite directions.
Manhattan lattice, when turned 45 degrees, can be viewed as two crossed Galton boards (Figure 3.8(a)) when we place scatterers (coins) only at the nodes where lines with the same color cross. In terms used

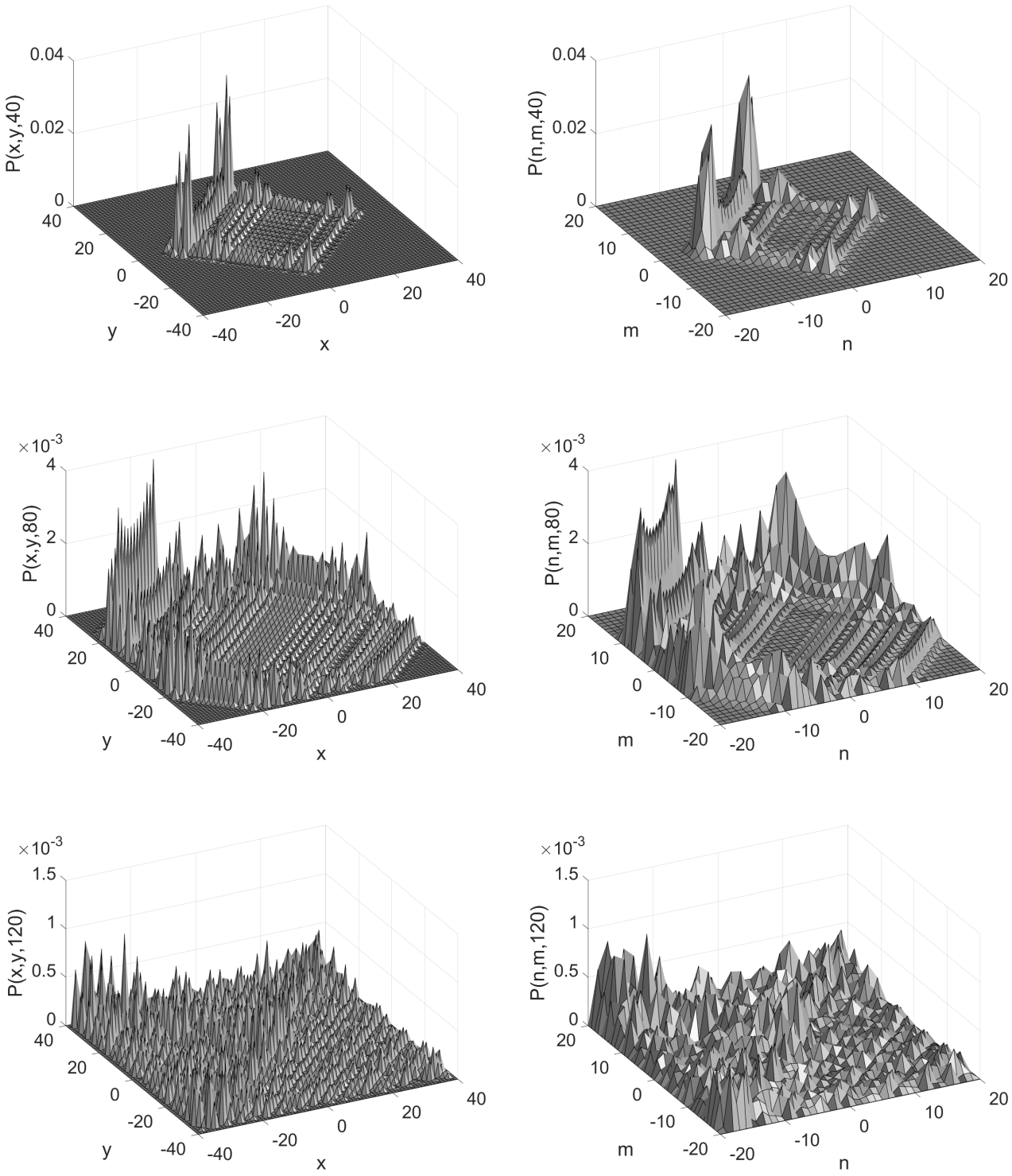

Figure 3.4: Hadamard walk with absorbing boundaries after 40, 80 and 120 steps with the initial state $\psi_1 = \frac{1}{\sqrt{2}}(0, 1, \mathrm{i}, 0)$. The probability distribution with respect to the Manhattan lattice is on the left, the corresponding probability distribution on the Cartesian lattice is on the right.

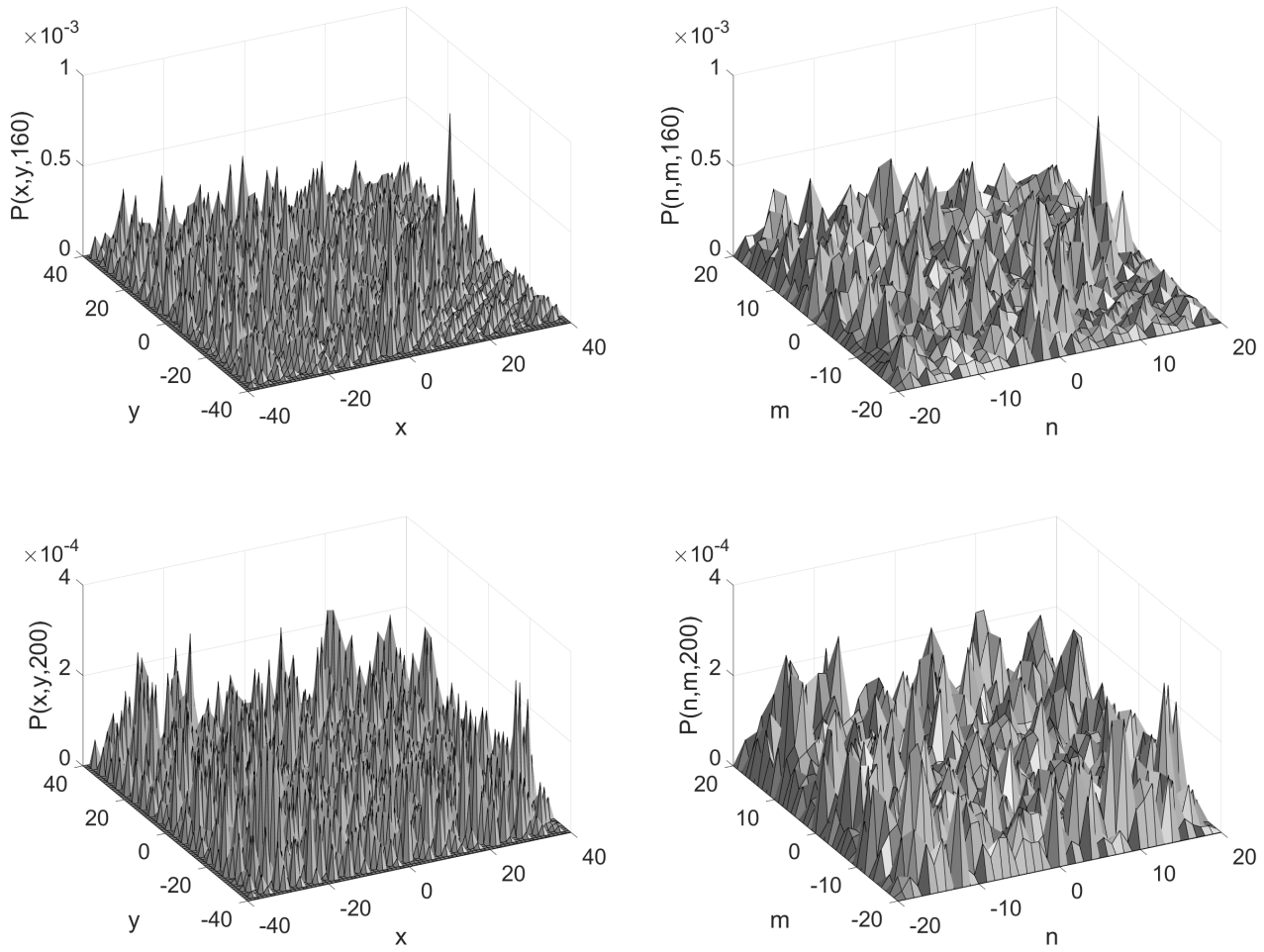

Figure 3.5: Hadamard walk with absorbing boundaries after 160 and 200 steps with the initial state $\psi_1 = \frac{1}{\sqrt{2}}(0, 1, \mathrm{i}, 0)$. The probability distribution with respect to the Manhattan lattice is on the left, the corresponding probability distribution on the Cartesian lattice is on the right.

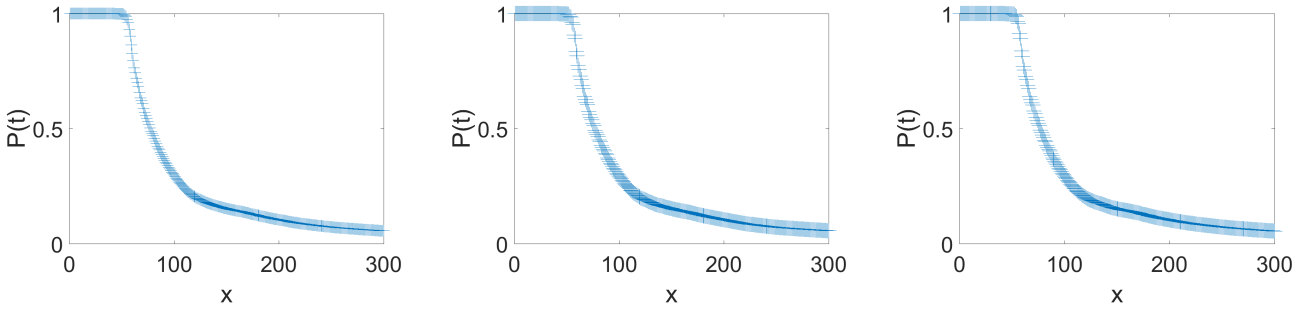

Figure 3.6: Dependence of the survival probability on the choice of the initial state. We have used the 40×40 Manhattan lattice and the initial states given by (3.41). We see that the choice of the initial state does not significantly affect the survival probability.

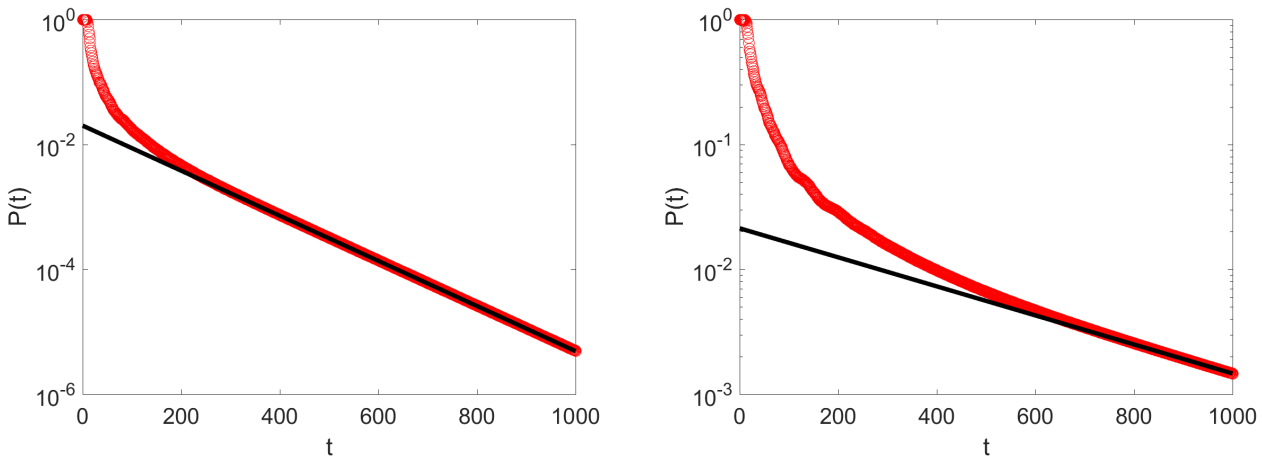

Figure 3.7: The survival probability on the log scale on the 9×9 Cartesian lattice for the Hadamard walk (on the left) and for the quantum walk with the rotation coin $C_R(\pi/3)$ (on the right). The red points represent the survival probability whereas the black line corresponds to the estimate (3.50)

above it means that in each cell the coins C_1 and C_4 are identity matrices (see (3.2)).
Let us now suppose that at the two other nodes we use the Hadamard matrices. The probability distribution of the resulting quantum walk is depicted in Figure 3.8(b). Obviously, this quantum walk takes the form of two probability distributions of independent one-dimensional quantum walks propagating in the opposite directions due to the orientation of the edges. At this point we note that straightforward extension to the model of two interacting one-dimensional quantum walks is not possible as a consequence of the opposite orientation of the time axis. Using a scatterer at the red-black crossing would lead to the particle moving back in time.

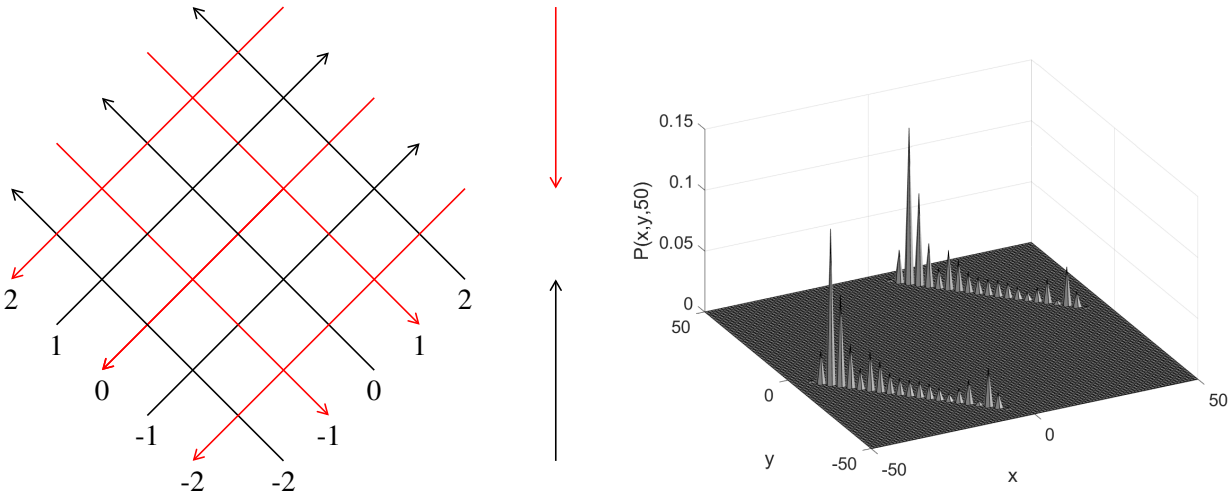

Figure 3.8: Manhattan lattice as two crossed Galton boards (on the left) and the probability distribution of the Hadamard quantum walk on the two crossed Galton boards with the initial state $\psi = \frac{1}{\sqrt{2}}(0,1,1,0)$ (on the right).

Chapter 4

Inhomogeneous quantum walk on the Manhattan lattice

Let us now turn to the inhomogeneous quantum walks on the Manhattan lattice which represent a generalization of the homogeneous model described above. We expect more interesting behaviour with respect to the effect of localization that has proven to be trivial in the homogeneous case.
In the following we only consider spatially inhomogeneous quantum walk, i. e. we generate one configuration of the Manhattan lattice at the beginning and do not change this configuration during the time evolution. We restrict ourselves to one choice of the square Manhattan lattice with absorbing boundaries where we consider three types of coins that are placed at the nodes of the lattice according to the prescribed probabilities. This case of the inhomogeneous quantum walks does not enable us to employ the Fourier transform used in the previous chapters. Therefore, we resort to numerical simulations.
At this point we note that we can also consider time-inhomogeneous quantum walk, where we generate new configuration of the underlying lattice at each time step. However, this concept is beyond the scope of this thesis.

4.1 Absorbing boundaries

In the following we consider quantum walks on the Manhattan lattice driven by three types of coins: the Hadamard coin H, the reflection matrix R representing the scatterer in the classical case and the identity matrix I which corresponds to the unhindered propagation of the particle. Due to the orientation of the edges, each of the coins takes four different forms (3.2) dependent on the position on the lattice; explicitly

$$H_1 = \frac{1}{\sqrt{2}}\begin{pmatrix} 1 & 0 & 0 & 0 \\ 0 & 1 & 1 & 0 \\ 0 & 1 & -1 & 0 \\ 0 & 0 & 0 & 1 \end{pmatrix}, \; H_2 = \frac{1}{\sqrt{2}}\begin{pmatrix} 1 & 0 & 0 & 0 \\ 0 & 1 & 0 & 0 \\ 0 & 0 & 1 & 1 \\ 0 & 0 & 1 & -1 \end{pmatrix}, \; H_3 = \frac{1}{\sqrt{2}}\begin{pmatrix} 1 & 1 & 0 & 0 \\ 1 & -1 & 0 & 0 \\ 0 & 0 & 1 & 0 \\ 0 & 0 & 0 & 1 \end{pmatrix}, \; H_4 = \frac{1}{\sqrt{2}}\begin{pmatrix} -1 & 0 & 0 & 1 \\ 0 & 1 & 0 & 0 \\ 0 & 0 & 1 & 0 \\ 1 & 0 & 0 & 1 \end{pmatrix},$$

$$R_1 = \begin{pmatrix} 1 & 0 & 0 & 0 \\ 0 & 0 & 1 & 0 \\ 0 & 1 & 0 & 0 \\ 0 & 0 & 0 & 1 \end{pmatrix}, \quad R_2 = \begin{pmatrix} 1 & 0 & 0 & 0 \\ 0 & 1 & 0 & 0 \\ 0 & 0 & 0 & 1 \\ 0 & 0 & 1 & 0 \end{pmatrix}, \quad R_3 = \begin{pmatrix} 0 & 1 & 0 & 0 \\ 1 & 0 & 0 & 0 \\ 0 & 0 & 1 & 0 \\ 0 & 0 & 0 & 1 \end{pmatrix}, \quad R_4 = \begin{pmatrix} 0 & 0 & 0 & 1 \\ 0 & 1 & 0 & 0 \\ 0 & 0 & 1 & 0 \\ 1 & 0 & 0 & 0 \end{pmatrix}. \tag{4.1}$$

We use the same square $2N \times 2N$ Manhattan lattice with absorbing boundaries where N is even. The position space is given as a span $= \{|x, y\rangle \,|\, -N \leq x \leq N-1, -N \leq y \leq N-1\}$ and we assume the

boundary to be described by lines $x = -N,\ x = N - 1,\ y = -N$ and $y = N - 1$.
Let us denote by p_H the probability of using the Hadamard coin at the given vertex, by p_R the probability of placing the reflection coin and p_I denotes the probability of using the identity matrix on the given vertex.
Our aim now is to study the dependence of the localization on the above probabilities. From the relation for the asymptotic behaviour of the survival probability given by (3.50) follows that this probability decays exponentially for the evolution operators with the largest eigenvalues which are less than one in the absolute value. In the case of quantum walks discussed in this chapter we say that the quantum walk is localized if the largest eigenvalues in the absolute value is equal to one.

We have obtained some preliminary results using numerical simulations for one special choice of square 12×12 Manhattan lattice. The Figures 4.1, 4.2 depict the dependence of the largest eigenvalues in the absolute value of the evolution operator U on the choice of the probability p_R in the case of 12×12 square Manhattan lattice. The red lines represent the histogram in the classical case in which the discussed absolute values of the eigenvalues of the step operator take only values 0 or 1. The black lines correspond to its quantum counterparts with all of the values of $|\lambda_{max}|$ equal or close to 1. The probability p_R in the plots was set to 9/10 in the first histogram, then decreasing by 1/10 in the following plots. For each of the probabilities we generated 150 configurations of the Manhattan lattice. In the classical case, the rest of the nodes without the reflection are left with the identity matrix. On the contrary, in the quantum case we placed the Hadamard matrices on the rest of the nodes with probability $1 - p_R$.
Notice that the distribution of the $|\lambda_{max}|$ in the classical case correspond well with the quantum case meaning that the number of localized walks is approximately the same for both the classical and quantum walks in each of the plots. Based on these results, we infer a hypothesis that localization depends crucially on the probability p_R.
We note that in case of $p_R = 0$, $p_H = 1$ (is not included in the plot) all of the $|\lambda_{max}|$ equal to 0.98947270362 in the quantum case which is exactly the largest eigenvalue in the absolute value in case of the corresponding 8-state quantum walk on the Cartesian lattice discussed in the previous chapter.
We also note that for the probability p_R greater than 1/2 the trapped walks prevail which is consistent with the result presented in [5] that for the discussed probability greater than 1/2 all of the classical walks are bounded.

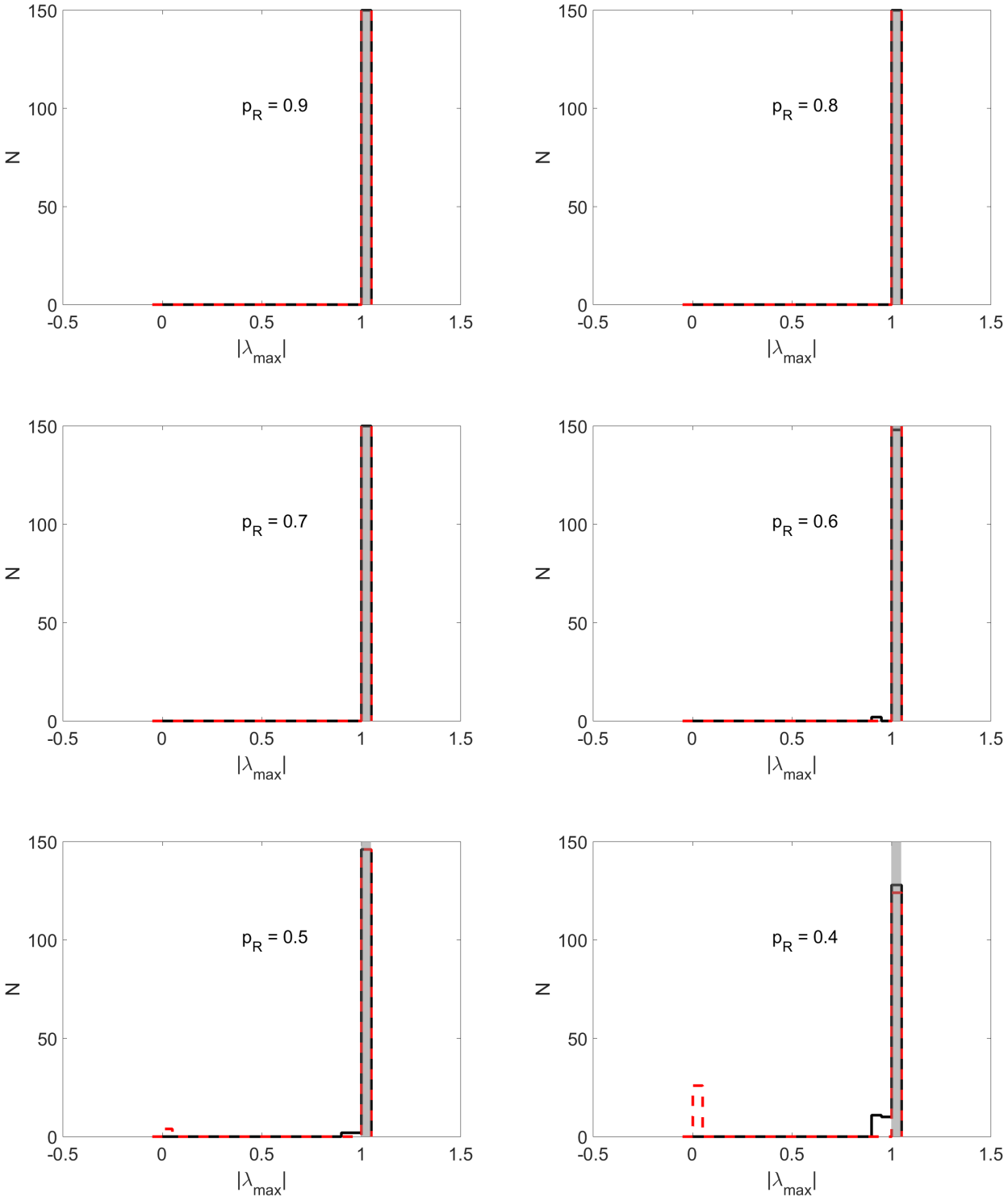

Figure 4.1: Histograms depicting the dependence of the largest eigenvalue in the absolute value $|\lambda_{max}|$ of the evolution operator on the probability p_R in the case of the classical random walk (red lines) and the quantum walks (black lines). The numerical simulation was done for square 12×12 Manhattan lattice with absorbing boundaries. The grey bin marks the $|\lambda_{max}| = 1$ which is responsible for the localization.

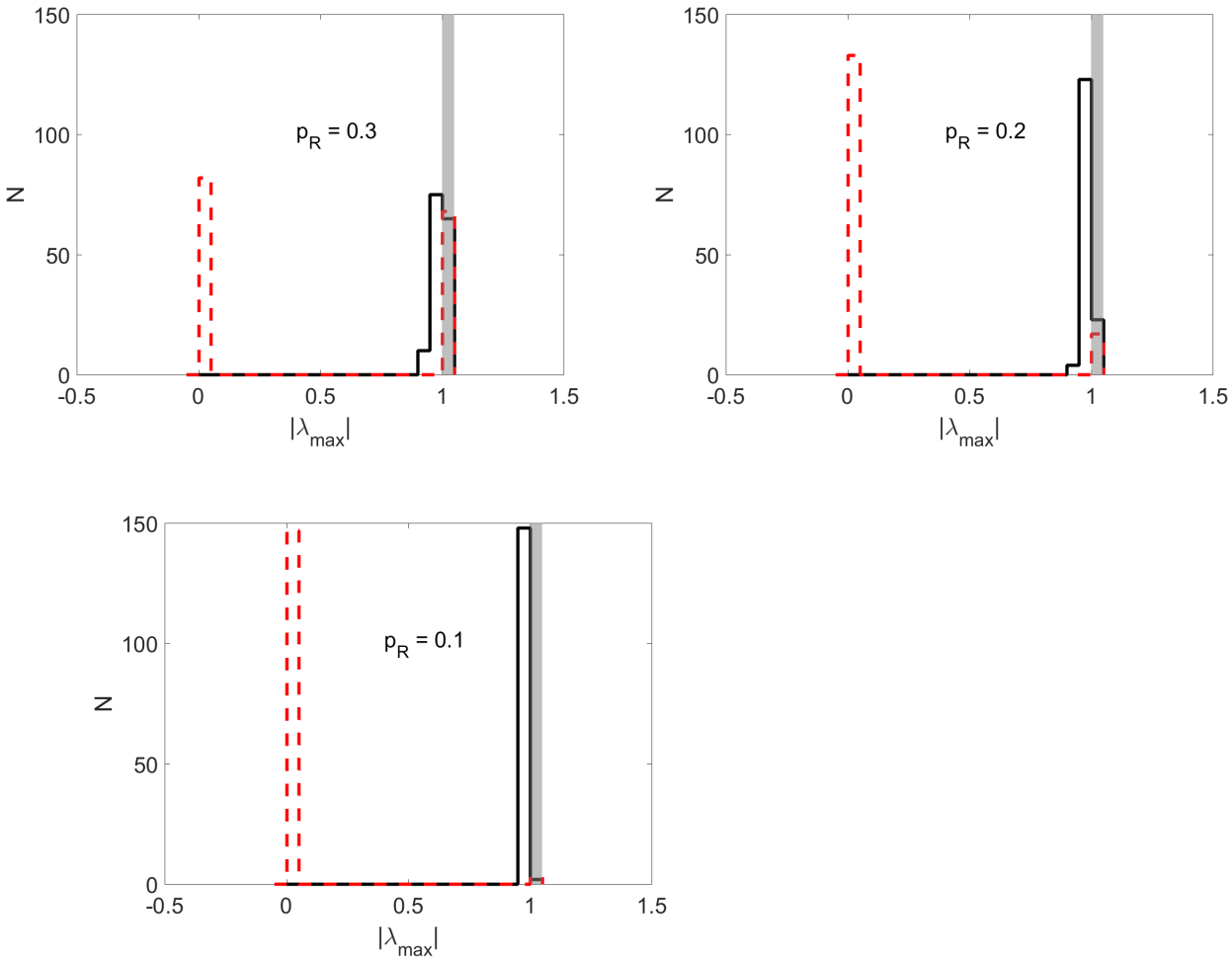

Figure 4.2: Continuation of Figure 4.1.

Conclusion

In this thesis we have focused on quantum walks on the Manhattan lattice. In the first chapter we have introduced the concept of two-dimensional quantum walks and summarized some its properties relevant to the rest of the thesis. The second chapter dealt with some of the properties of the classical random walks on the Manhattan lattice.
The concept of homogeneous quantum walks on the Manhattan lattice was introduced in the third chapter. We have successfully mapped the problem of the analysis of this type of quantum walk on the task of studying 8-state quantum walk on the Cartesian lattice and analysed the time evolution of the latter. We focused especially on the effect of trapping; having imposed conditions on the spectrum of the evolution operator in the Fourier domain we obtained SU(2) form of the general trapping coin and observed that the trapping effect in homogeneous quantum walks on the Manhattan lattice is trivial. We have also considered special cases of these homogeneous quantum walks driven by the Hadamard coin and the rotation matrix. The spectrum of these quantum walks have been obtained. We have also observed that the decay of the probability of being at the origin at time t suggests transience of the Hadamard walk.
The second part of the third chapter was devoted to the quantum walk on the finite Manhattan lattice. We have estimated numerically the rate of decay of the survival probability in the case of absorbing boundary conditions and commented on some special cases of quantum walks with periodic boundaries.
In the last chapter we touched upon the inhomogeneous quantum walks on the Manhattan lattice. We only considered one specific choice of the 12×12 square Manhattan lattice with absorbing boundaries and quantum walks homogeneous in time with spatial disorder. From the preliminary results obtained numerically we infer that the localization effect depends crucially on the probability p_R of using the reflection on the given node in both the classical and quantum case.

There remain many interesting open questions. The effect of localization in the spatially inhomogeneous case considered in the last chapter is to be analysed for bigger size of the Manhattan lattice and more general choice of the coin operator.
We note that we can also consider quantum walks inhomogeneous in time, where we generate new configuration of the Manhattan lattice at each time step. These two models that are analogous to static and dynamical percolations will be the subject of our further study.

Bibliography

[1] Y. Aharonov, L. Davidovich, and N. Zagury. Quantum random walks. *Phys. Rev. A*, 48:1687–1690, 1993.

[2] D. Meyer. From quantum cellular automata to quantum lattice gases. *J. Stat. Phys.*, 85:551–574, 1996.

[3] L. Grover. A fast quantum mechanical algorithm for database search. In *Proceedings of the Twenty-Eighth Annual ACM Symposium on the Theory of Computing, Philadelphia, Pennsylvania, USA, May 22-24, 1996*, pages 212–219, 1996.

[4] K. Manouchehri and J. Wang. *Physical Implementation of Quantum Walks*. Springer Publishing Company, Berlin, 2014.

[5] E. J. Beamond, A. L. Owczarek, and J. Cardy. Quantum and classical localisation and the Manhattan lattice. *Journal of Physics A*, 36:10251, 2002.

[6] A. Ambainis, E. Bach, A. Nayak, A. Vishwanath, and J. Watrous. One-dimensional quantum walks. In *Proceedings of the Thirty-third Annual ACM Symposium on Theory of Computing*, STOC '01, pages 37–49, New York, NY, USA, 2001.

[7] P. W. Anderson. Absence of diffusion in certain random lattices. *Phys. Rev.*, 109:1492–1505, 1958.

[8] A. Joye and M. Merkli. Dynamical Localization of Quantum Walks in Random Environments. *J. Stat. Phys.*, 140:1025, 2010.

[9] N. Konno. Localization of an inhomogeneous discrete-time quantum walk on the line. *Quantum Inf Process*, 8:405, 2009.

[10] A. Kempf and R. Portugal. Group velocity of discrete-time quantum walks. *Phys. Rev. A*, 79(5):052317, 2009.

[11] N. Inui, N. Konno, and E. Segawa. One-dimensional three-state quantum walk. *Phys. Rev. E*, 72:056112, 2005.

[12] M. Štefaňák, B. Kollár, T. Kiss, and I. Jex. Full revivals in 2D quantum walks. *Physica Scripta Volume T*, 140(1):014035, 2010.

[13] K. Watabe, N. Kobayashi, M. Katori, and N. Konno. Limit distributions of two-dimensional quantum walks. *Phys. Rev. A*, 77(6):062331, 2008.

[14] B. Kollár, T. Kiss, and I. Jex. Strongly trapped two-dimensional quantum walks. *Phys. Rev. A*, 91(2):022308, 2015.

[15] G. Pólya. Über eine Aufgabe der Wahrscheinlichkeitsrechnung betreffend die Irrfahrt im Straßennetz. *Math. Ann.*, 84(1-2):149–160, 1921.

[16] M. Štefaňák, T. Kiss, and I. Jex. Recurrence of biased quantum walks on a line. *New Journal of Physics*, 11(4):043027, 2009.

[17] M. Štefaňák, J. Novotný, and I. Jex. Percolation assisted excitation transport in discrete-time quantum walks. *New Journal of Physics*, 18(2):023040, 2016.

[18] R. Portugal. *Quantum walks and search algorithm*. Springer, New York, 2013.